Functional Properties of Sarcoplasmic Reticulum Ca 2+ -ATPase after Proteolytic Cleavage at Leu 119 -Lys 120 , Close to the A-domain

Guillaume Lenoir, Martin Picard, Carole Gauron, Cédric Montigny, Pierre Le Marechal, Pierre Falson, Marc Le Maire, Jesper Møller, Philippe Champeil

Functional properties of sarcoplasmic reticulum Ca^{2+}-ATPase after proteolytic cleavage at Leu^{119}-Lys^{120}, close to the *A*-domain.

Guillaume Lenoir[§], Martin Picard[§], Carole Gauron[§], Cédric Montigny[§], Pierre Le Maréchal[¶], Pierre Falson[§], Marc le Maire[§], Jesper V. Møller[*] and Philippe Champeil[§]

[§] Service de Biophysique des Fonctions Membranaires (DBJC, CEA), Unité de Recherche Associée 2096 (CNRS), LRA-17V and IFR-46 (Université Paris-Sud), CEA-Saclay, 91191 Gif-sur-Yvette Cedex (France),

[¶] Institut de Biochimie et Biophysique Moléculaire et Cellulaire, Equipe Chimie des Protéines, UMR CNRS 8619 and IFR-46, Université Paris Sud (Bat 430), F-91405 Orsay cedex (France), and

[*] Department of Biophysics, University of Aarhus, Ole Worms Allé 185, 8000 Aarhus C (Denmark).

Abbreviations: SR, sarcoplasmic reticulum; PK, proteinase K; TCA, trichloroacetic acid; PMSF, phenylmethylsulfonyl fluoride; SDS, sodium dodecyl sulfate; PAGE, polyacrylamide gel electrophoresis; Mops, 4-morpholinepropanesulfonic acid; DMSO, dimethyl sulfoxide; MALDI-TOF, matrix-assisted laser desorption ionization-time of flight; DM, β-D-dodecyl maltoside; $C_{12}E_8$, octaethylene glycol monododecyl ether; HPLC, high pressure liquid chromatography; TEMED, N,N,N',N'-tetramethylethylenediamine.

ABSTRACT *(208 words)*

By measuring the phosphorylation levels of individual proteolytic fragments of SERCA1a separated by electrophoresis after their phosphorylation, we were able to study the catalytic properties of a p95C/p14N complex arising from cleavage by proteinase K between Leu^{119} and Lys^{120}, in the loop linking the ATPase *A*-domain with the second transmembrane segment. ATP hydrolysis by the complex was very strongly inhibited, although ATP-dependent phosphorylation and the conversion of the ADP-sensitive E1P form to E2P still occurred at an appreciable rate. However, the subsequent dephosphorylation of E2P was inhibited to a dramatic extent, and this was also the case for "backdoor" formation of E2P from E2 and Pi. Concomitantly, E2P formation from E2 at equilibrium indicated little change in the apparent affinity for Pi or Mg^{2+}, while binding of ortho-vanadate was weaker. The p95C/p14N complex also had a slightly reduced affinity for Ca^{2+} and exhibited a reduced rate for its Ca^{2+}-dependent transition from E2 to E1. Thus, disruption of the N-terminal link of the *A*-domain with the transmembrane region seems to poise the conformational equilibria of Ca^{2+}-ATPase from the E1/E1P towards the E2/E2P states and to increase the activation energy for dephosphorylation of Ca^{2+}-ATPase, reviving the old idea of the *A*-domain being a phosphatase domain, part of the transduction machinery.

INTRODUCTION

Large scale relative movements of the three main sub-domains in the cytosolic head of P-type ATPases, as well as associated movements of the transmembrane segments to which these domains are connected, probably play a major role in the active transport mediated by these membrane proteins *(Toyoshima et al., 2000, 2002)*. We have therefore become interested in the functional effects of proteolytic disruption of the integrity of the loops connecting these various ATPase domains. For rabbit SERCA1a, a representative of P-type ATPases involved in Ca^{2+} transport into intracellular compartments, we have previously studied how Ca^{2+} transport and ATP hydrolysis are affected by proteolytic cleavage at a site located in the segment linking the *A*-domain with the third transmembrane segment, M3 (*Møller et al., 2002*). In that previous work, the proteolysis conditions had allowed us to obtain relatively large (milligram) amounts of fairly pure "p28N/p83C" peptide complexes, derived from ATPase by excision of a short $MAATE^{243}$ sequence from this segment, and procedures that previously had been developed to study the catalytic cycle of intact ATPase were used unaltered to study the properties of the proteolytic product. The results showed that the cleaved ATPase was deficient in Ca^{2+} transport but remained phosphorylatable by ATP in a manner indistinguishable from that of intact ATPase. A detailed study of the partial reactions revealed that a major defect resulting from proteolysis was the difficulty for the cleaved ATPase to enter what is known as the "E2P" state, i.e. the ADP-insensitive form of phosphoenzyme. This was true both when we tried to approach this state from the ADP-sensitive form of phosphoenzyme ("Ca_2E1P", whose conformational transition to E2P during normal turnover is associated with Ca^{2+} translocation) and when we tried to form it directly from the Ca^{2+}-free form of non-phophorylated ATPase ("E2", which in intact ATPase can be phosphorylated from Pi by the "backdoor" reaction, in the reverse direction). These data provided direct support for the view that the *A*-domain in P-type ATPases plays a critical role in the structural changes accompanying cation transport (*Møller et al., 2002*).

In the present work, we have aimed at studying whether SERCA1a function is

affected by proteolytic cleavage in another part of the link between the *A*-domain and the membrane. To do so, we again resorted to proteolytic attack by proteinase K, but instead of performing the proteolysis in the presence of Ca^{2+} and AMPPCP, as was previously done (*Møller et al., 2002*), we now treated the ATPase in the absence of Ca^{2+} and nucleotide: this is known to allow cleavage at Leu^{119}-Lys^{120}, in the segment linking the *A*-domain with the second transmembrane segment, resulting in the formation of complementary "p14N" and "p95C" peptides (*Juul et al., 1995*). In this case, however, proteolysis also simultaneously occurs at other sites, so that a mixture of peptides is formed, among which p95C is only present in relatively small amounts compared with p83C or residual intact ATPase. To study the catalytic properties of the p95C/p14N complex, we therefore had to resort to new procedures. We combined two types of established experiments: firstly, after phosphorylation of the various peptides we separated them by electrophoresis under conditions previously found to allow decent separation between fragments of large size and yet miminize dephosphorylation *(Sarkadi et al., 1986)*; secondly, we made use of various phosphorylation and dephosphorylation protocols previously used to characterize kinetically the individual steps in the catalytic cycle of heterologously expressed ATPase mutants. This allowed us to simultaneously study to what extent the p95C and the p83C peptides were phosphorylated or dephosphorylated under various situations, and to compare their properties with those of residual intact ATPase. Results concerning the p83C/p28N complex were consistent with those that we had previously obtained with conventional methods *(Møller et al. 2002)*. The present paper therefore focuses on the catalytic properties of the p95C/p14N complex resulting from cleavage of the Lys^{119}-Leu^{120} bond: we find that following this cleavage Ca^{2+}-ATPase turnover is severely perturbed, but in a manner quite different from that obtained by excision of the ^{238}MAATE sequence in the peptide chain linking the A domain with M3. These results make it possible to get a better understanding of the role of the *A*-domain for the intermediary processes involved in Ca^{2+}-transport.

METHODS

Proteolysis by proteinase K (PK). For controlled proteolysis of sarcoplasmic reticulum (SR) Ca^{2+}-ATPase, SR membranes *(Champeil et al., 1985)* were suspended at a concentration of 2 mg protein/ml in a 100 mM Mops-NaOH medium (pH 6.5) containing 5 mM Mg^{2+} and 0.5 mM EGTA, and treated with PK at 0.03 mg/ml, generally for 15-16 min at 20°C. Proteolysis was stopped by adding 0.5 or 1 mM PMSF (as well as 0.6 mM Ca^{2+} in some cases) and storing the samples on ice for 10 min. For some of the phosphorylation experiments, viz. those involving [γ-^{32}P]ATP, the preparation with inactivated PK was used without further treatment as detailed below. For other phosphorylation experiments, viz. those involving [^{32}P]Pi which were best performed with a higher concentration of protein than those involving [γ-^{32}P]ATP, a large batch of PK-treated concentrated membranes was first prepared; for this purpose, 9 ml of PK-treated membranes at 2 mg protein/ml was treated with PK and PMSF as above, and then pelleted (after adding 0.3 M sucrose, 20 mM Tes-Tris at pH 7.5 and 0.6 mM Ca^{2+}, to protect the ATPase from EGTA-dependent denaturation during centrifugation). Membranes were then resuspended at about 20 mg/ml protein (judging from OD_{280nm} of an aliquot solubilized in SDS) in 0.3 M sucrose, 100 mM KCl and 20 mM Tes-Tris (pH 7.5), before freezing in liquid nitrogen and storage at –80°C until subsequent use. When SR vesicles were treated this way, SDS-PAGE revealed essentially the same pattern as shown in lane 8 of Fig 1, except that in this case, of course, the soluble p29/30 fragments were absent from the resuspended pellet (data not shown).

Phosphorylation and dephosphorylation. Phosphorylation from [γ-^{32}P]ATP of ATPase fragments was generally measured on ice, by adding 5 μM [γ-^{32}P]ATP (at 0.5 mCi/μmol) to PK-treated membranes suspended in buffer A (100 mM KCl, 5 mM Mg^{2+} and 50 mM Mops-Tris, adjusted to pH 7.0 at room temperature), supplemented with various concentrations of Ca^{2+} (or a Ca^{2+}/EGTA buffer). The protein concentration in these experiments was 0.2 mg/ml,

i.e. the proteolyzed sample was diluted 10-fold into the final phosphorylation medium, which was typically 600 µl per sample. When desired, ATPase dephosphorylation was subsequently triggered by adding EGTA and the appropriate additive, with only small dilution (see below for details). In some cases, phosphorylation was also measured after a few milliseconds reaction at 20°C, with a Biologic QFM5 quenched-flow apparatus.

Phosphorylation from [^{32}P]Pi of ATPase fragments was measured by adding [^{32}P]Pi (at 0.5 mCi/µmol), generally at 200 µM, to concentrated PK-treated membranes suspended in buffer B (25% DMSO (v/v), 10 mM Mg^{2+}, 1 mM EGTA and 50 mM Mops/Tris, adjusted to pH 7.0 at room temperature). The protein concentration in these experiments was generally 1-2 mg/ml, and the protein was typically suspended in 60 µl per sample. When desired, ATPase dephosphorylation was then triggered either by adding excess non-radioactive Pi (resulting in only little dilution; experiments of this kind were performed at 20 °C), or by ten-fold dilution of the phosphorylated sample into a DMSO-free, KCl- and ATP-containing buffer (experiments of this kind were performed on ice, see below).

In all cases the reaction was stopped by acid quenching with TCA (or in some cases PCA) and phosphoric acid, at final concentrations of 500 mM and 30 mM, respectively (typically in a total volume of 900 µl). Generally, while a small aliquot of the sample was filtered through Millipore HA or Gelman A/E filters for control measurements, most of the quenched sample, previously left on ice for 20 minutes, was pelleted by centrifugation (15,000 rpm for 25 minutes, 4°C). The supernatant was sucked off and replaced by an equivalent volume of acid solution (diluted 10-fold compared to the final quenching solution), and the sample was centrifuged as before. After removal of the second supernatant, the pellet was resuspended in 250 µl of a sample buffer containing 2 % SDS, 10 mM EDTA, 150 mM Tris-HCl (at pH 6.8), 16 % (v/v) glycerol (or 8 M urea in some cases), 0.8 M β-mercaptoethanol and 0.04 % bromophenol blue, by vortexing for one minute (thorough vortexing was found to be critical for reproducible resuspension of the acid-treated pellet); 20 µl aliquots were then loaded onto gel for electrophoretic separation as described below.

Electrophoretic separation according to Sarkadi. This was performed according to protocols previously described (*Sarkadi et al., 1986, 1988; Menguy et al., 1998; Tsivkovskii et al., 2002;* see also *Echarte et al., 2001*, for a related approach), but with some modifications. The stacking gel contained 4 % acrylamide (with an acrylamide to bisacrylamide ratio of 29 to 1), 65 mM Tris-H3PO4 pH 5.5, 0.1 % SDS, 2 % ammonium persulfate and 0.1 % TEMED. The separating gel was a continuous 7 % gel, containing 65 mM Tris phosphate pH 6.5, 0.1 % SDS, 0.4 % ammonium persulfate and 0.05 % TEMED. Unless otherwise indicated, gels were run in the cold room. The pre-cooled running buffer contained 170 mM Mops/Tris pH 6.0 and 0.1 % SDS; it was kept under stirring during electrophoresis in order to prevent heating of the gels. Electrophoresis lasted about 3 h, with a current intensity set constant to 10 mA/gel (70-80 V). Gels were then stained and fixed for 10 minutes in 40 % methanol, 10 % acetic acid and 0.1 % Coomassie Blue R250. Destaining was carried out in 10 % acetic acid, 10 % methanol and 1 % glycerol within less than one hour, and the gels were then dried overnight between two sheets of cellophane paper, prior to exposure to a phosphor screen the next morning. Radioactivity was revealed with a STORM 860 PhosphorImager (Molecular Dynamics) and quantified by comparison with known amounts of [γ-^{32}P]ATP or [^{32}P]Pi. In some cases, phosphorylated samples were also run in a Laemmli-type system (*cf. Juul et al., 1995*), in order to compare the efficiency of the two systems for recovery of phosphorylated fragments after electrophoretic migration. *Figure "0" of the Supplemental Data section* shows that the large C-terminal fragments obtained after Ca^{2+}-ATPase treatment with PK can indeed be clearly separated by Sarkadi gels, run in the cold room or at 20°C. Recovery on the gel of the ^{32}P initially bound covalently to the fragments is, as expected, much better than in the alkaline Laemmli gels, being higher than 50 %, as judged either from PhosphorImager direct counting of a similar aliquot of the resuspended pellet (without electrophoresis, not shown), or from parallel experiments with intact SR ATPase whose phosphorylation level can be independently measured by direct

filtration. This fair recovery of phosphorylated protein after electrophoresis is similar to that reported after electrophoresis with Weber and Osborn gels. At least in our hands, the Weber and Osborn procedure was slower and had poorer resolution (*data not shown*).

Solubilization and elution of the p95C/p14N complex in the presence of detergent. After proteolysis under usual conditions, except for the absence of Mg^{2+}, and PMSF addition, as well as under identical conditions but in the absence of PK treatment (for control), samples were cooled to 4°C, and 10 mg/ml DM (final concentration) was added together with 1 mM Ca^{2+}, to solubilize most of the protein without too much denaturation. Samples (180 µl, containing about 300 µg of protein) were centrifuged to eliminate non-solubilized material (Beckman TL 100 centrifuge, TLA100 rotor, 50,000 rpm for 5 min at 8°C) and the supernatant was loaded on a TSK 3000SW HPLC column for size exclusion chromatography and delipidation in the presence of DM. The eluant in the column contained 50 mM Mops-NaOH at pH 7, 50 mM NaCl and 0.4 mg/ml DM. PK-treated samples displayed an elution pattern with a main peak at essentially the same position as the one where uncleaved monomeric Ca^{2+}-ATPase elutes (*Champeil al., 2000*), and this peak was collected (about 0.75 ml); it was then diluted with an equal amount of 50 mM MOPS-Tris(pH 7) and 0.4 mg/ml DM, to reduce the salt content, and concentrated to about 50 µl with YM100 Centricon device (Beckman Avanti J20XP centrifuge, JA12 rotor, 1000 g for 30 min at 4°C). An aliquot of the sample was loaded onto a 12 % Laemmli gel for SDS-PAGE, Western Blotting on Immobilon membranes and immunodetection with an antibody against residues 1-15 of Ca^{2+}-ATPase (cf. *Møller et al., 2002*) (see *bottom Panel in Fig 1*). Another aliquot was used for MALDI-TOF analysis of p14N without further separation (see below), while a third aliquot (about 10 µg) was loaded on a second SDS-PAGE 12 % gel, submitted to electrophoresis and stained; the band corresponding to p14 was then cut off for subsequent treatment with trypsin and MALDI-TOF analysis of the resulting peptides (see below).

Mass spectrometry analysis .

For analysis of the HPLC-purified protein fragment, 1 µl of the delipidated sample in its detergent environment was mixed with 1 µl of cytochrome c from bovine heart, corresponding to 500 femtomoles. Two microliters of saturated solution of sinapinic acid in 30 % acetonitrile and 0.3 % trifluoroacetic acid were added, and 1 µL of this mixture was loaded on the MALDI target. Spectra were acquired on a MALDI-TOF spectrometer (Perseptive Biosystems, Voyager STR-DE) equipped with a nitrogen laser (337 nm), in linear mode using delayed extraction, with an accelerating voltage of 20 kV. The cytochrome c in the loaded sample provided an internal calibration.

For analysis of the peptides resulting from trypsinolysis of the p14 band, this band was first treated with 250 ng of trypsin, after removal of stain and SDS as previously described *(Shevchenko et al., 1996*). One microliter of the tryptic mixture was mixed with 1 µl of saturated solution of α-cyanohydroxycinnamic acid in 50 % acetonitrile and 0.3 % trifluoroacetic acid, and the mixture was loaded on the MALDI target. Spectra were obtained in reflector mode using delayed extraction, with an accelerating voltage of 20 kV. External calibration was performed with a mixture of 6 peptides covering the range 900-3600 Da.

Edman degradation analysis and other methods

After SDS-PAGE separation of PK-treated fragments on an 8 % Laemmli gel (with 1 mM thioglycolate in the running buffer), the N-terminus of the blotted p95C fragments was sequenced using a Procise (Applied Biosystems) protein sequencer.

Low concentrations of free Ca^{2+} were obtained by buffering with EGTA, using the following apparent dissociation constants for Ca^{2+} and Mg^{2+} at pH 7: $Kd_{Ca.EGTA} \sim 0.4$ µM and $Kd_{Mg.EGTA} \sim 25$ mM.

Structures were visualized using the SwissPDB Viewer (Guex & Peitsch, 1997; http://www.expasy.org/spdbv/).

RESULTS

Multiple fragmentation of Ca^{2+}-ATPase treated with proteinase K (PK), with formation of a p95C/p14N complex in the absence of Ca^{2+}, and assay of phosphorylatable proteolytic peptides with Sarkadi gels.

The typical pattern of ATPase proteolysis in the presence or absence of Ca^{2+}, as deduced from gel electrophoresis on Laemmli gels, is shown in the top panel of *Fig 1*. Lanes 2-5 in this Panel show that, as previously documented, treatment of SR vesicles with proteinase K in the presence of Ca^{2+} gives rise to a number of well characterized initial products, comprising membraneous peptides derived from either the N-terminal (p28N) or the C-terminal part (p83C and p19C) of the ATPase, together with water-soluble p29/30 fragments derived from the central nucleotide binding domain (*Juul et al., 1995; Champeil et al., 1998*). The Thr^{242}-Glu^{243} peptide bond whose cleavage results in production of the p28N and p83C peptides is indeed found to be in an exposed position in crystallized Ca^{2+}-bound ATPase *(Toyoshima et al.., 2000)*, consistent with its accessibility to proteolysis. In the absence of Ca^{2+}, fragments with the same apparent mass as the p83C and p28N band again show up (lanes 6-9 in *Fig 1A*), but in this case a new band with a higher molecular mass, the "p95" peptide is also transiently formed in the first 15 min, together with a new p14 band, but both bands are essentially completely degraded after 60 min (compare lanes 6-9 with lanes 2-5, and see similar results in *Juul et al., 1995 and Danko et al., 2001a*). This p95 band represents a C-terminal peptide that previously was found to arise from ATPase cleavage at Leu^{119}-Lys^{120} (*Juul et al., 1995)*, and by Edman degradation analysis we here confirmed this assignment (data not shown). The complementary N-terminal fragment, p14N, clearly visible on lane 8 in Fig 1 (but not after cleavage in the presence of Ca^{2+}), was previously designated as p14a in *Juul et al., 1995* (note that in the legend to Table I of that paper, it was erroneously indicated that this peptide corresponds to residues 1-19, instead of 1-119). Thus, the absence of Ca^{2+} appears to result in an increased susceptibility of the ATPase chain to PK cleavage at

Leu^{119}-Lys^{120}. For convenience, the central part of Figure 1 (adapted from Fig 3 in *Juul et al., 1995*) recalls the position of the main identified cleavage points on Ca^{2+}-ATPase, as well as some of the resulting peptides.

For functional studies, the question whether the complementary p14N and p95C fragments arising from the above-described cleavage remain associated in the membrane is an important issue. After treatment with PK, we solubilized the treated SR membranes with a mild detergent and chromatographed the solubilized sample on an HPLC size exclusion column in the presence of detergent. By both Western blotting and Coomassie blue staining, we found that the small p14N peptide indeed elutes at the same position where monomeric intact ATPase normally elutes (*bottom Panel in Figure 1).* Furthermore, p95C and p14N are present in the monomeric fractions in amounts consistent with the formation of a stoichiometric complex *(Fig 1bis* in the Supplemental Data section), suggesting that the two ATPase fragments resulting from cleavage at Leu^{119}-Lys^{120} remain closely associated despite the presence of detergent, as was previously demonstrated for the two ATPase fragments resulting from cleavage at Thr^{242}-Glu^{243}, that remain associated in a "p83C/p28N complex" *(Møller et al., 2002*). We therefore consider it likely that the former fragments also remain associated in the membrane after cleavage, hence our designation of these fragments in the remainder of this paper as a "p95C/p14N complex".

After treatment with PK for 15 minutes in the absence of Ca^{2+}, the amount of p95C peptide formed is comparable to that of undegraded ATPase, but smaller than the amount of p83C. After longer proteolysis periods, secondary cleavage sites evidently result in degradation of the primary products, p83C and p95C, giving rise to e.g. soluble p29/30 fragments already after 15 minutes. Thus, in PK-treated membranes, p95C/p14N is present together with p83C/p28N complexes, residual intact ATPase, and complexes resulting from more extensive proteolysis. The cartoon in the top part of *Fig 1ter in the Supplemental Data section* illustrates this, as well as the possible existence of complexes consisting of p83C, p14N and p14b (residues 120-242, *Juul et al. 1995*). By Western blotting with various

antibodies, we ascertained that the "p83C" band was not contaminated with the N-terminal fragment of similar mass ("p81N") that might have resulted from ATPase cleavage around residues 734-747 (see *Fig 1ter of the Supplemental Data section*).

We checked that after cleavage in the absence of Ca^{2+}, the N-terminal peptide formed, p14N, does have its C-terminal end at Leu^{119}, i.e. that proteinase K has not cleaved off a few more residues on the C-terminal side of this peptide. Mass spectrometry analysis showed that the 1-119 peptide is indeed not subject to further degradation (*Fig 1quater of the Supplemental Data section*), and simultaneously confirmed that, as previously established *(Tong, 1977),* the N-terminus of Ca^{2+}-ATPase is acetylated.

To study phosphorylation of our Ca^{2+}-ATPase fragments, we have adopted a moderately acidic gel electrophoresis system that previously has been described not only to retain the ability to resolve protein fragments of relatively similar molecular masses as efficiently as the Laemmli system, but also to allow phosphorylated P-type ATPases or fragments to remain phosphorylated during electrophoretic migration (*Sarkadi et al., 1986, 1988)*. We have been able to fully confirm the value of this SDS-PAGE system (*see Methods and Fig "0" in the Supplemental Data section*). The proteolytic peptides in the PK-treated SR membranes, submitted to phosphorylation according to various protocols, followed by acid quenching and resuspension in SDS, could be clearly separated without much loss of the covalently bound ^{32}P (less than half of the radioactivity was lost from the phosphorylated fragments, see Methods), and with higher resolution than by the Weber and Osborn procedure commonly used for revealing phosphorylated P-type ATPases (*data not shown*). In the following, we have therefore combined the use of such Sarkadi gels with the use of various phosphorylation and dephosphorylation protocols previously developed to study individual steps in the catalytic cycle of either SR intact Ca^{2+}-ATPase or expressed wild-type or mutant ATPase *(e.g. Clarke et al., 1989; Andersen & Vilsen, 1992; Sørensen et al., 1997)*.

The p95C/p14N complex can be phosphorylated from [γ-^{32}P]ATP at a relatively high rate, but dephosphorylates very slowly, even in the presence of ADP.

We first investigated the kinetics of Ca^{2+}-dependent phosphorylation from ATP of the proteolytic peptides. *Fig 2* shows the result of an experiment in which PK-treated SR vesicles, equilibrated in the presence of Ca^{2+}, were reacted with [γ-^{32}P]ATP at 20°C for short periods of time (milliseconds) before acid quenching and electrophoresis in the presence of SDS. PhosphorImager analysis of the ^{32}P-labelled gel (Figure 2A) revealed that besides residual intact ATPase, ^{32}P was retained to a significant extent only by the large p95C and p83C proteolytic fragments, as expected on the basis of previous experiments performed at steady-state (*Juul et al., 1995; Møller et al., 2002*), and that phosphorylation of the p95C fragment still occurred at a fast rate on the second time scale. The final phosphorylation levels were similar, as shown (in Panel B) by dividing the number of pmol of ^{32}P associated with each band by the extent of Coomassie Blue staining of the corresponding lane. This also allowed us to take into account any small difference in the total amount of protein loaded onto each lane (Panel C) that could be due to a slightly variable recovery of the acid-precipitated proteins. Although these final levels are subject to a number of uncertainties (e.g. spillover of the heavily labelled bands onto the fainter ones nearby) or biases (e.g. differences in the molecular weight of the various fragments considered or in their ability to bind Coomassie Blue), it is clear from the result that the two C-terminal peptide fragments, p95C and p83C, were phosphorylated to a high level, like that of intact ATPase. As concerns the p95C fragment, its rate of phosphorylation remained quite fast (although 3-fold slower than that of intact ATPase). In the absence of Ca^{2+}, essentially no phosphorylation from ATP showed up (lane 2), as expected. The reaction of phosphorylation from ATP in the p95C/p14N complex (the "Ca_2E1 to Ca_2E1P" transition) therefore appears not to be very different from that of intact ATPase or the p83C/p28N complex.

In separate experiments, performed on ice for convenience, steady state phosphorylation levels revealed a fairly similar dependence on free Ca^{2+} for intact ATPase

and the proteolytic peptides (*Fig 2bis in the Supplemental Data section)*. Note, however, that this is only an apparent affinity; and the "true" affinity of the peptides will be discussed later.

In contrast to this quasi-normal behaviour for the phosphorylation reaction, we found that the three phosphorylatable bands present in PK-treated membranes dephosphorylate at very different rates after initial phosphorylation from [γ-^{32}P]ATP. In the experiment shown in *Fig 3*, which was performed on ice, phosphorylation of the p95C/p14N complex (now measured on a time scale of seconds) was again comparable to that of intact ATPase and p83C/p28N (lanes 2-4), but p95C dephosphorylated very slowly, even more slowly than p83C (whose dephosphorylation was itself much slower than that of intact ATPase, as previously demonstrated in *Møller et al., 2002).* This was the case both when dephosphorylation was triggered by addition of EGTA and excess non radioactive MgATP in the presence of an ATP regenerating system (to reduce the ADP content as much as possible, lanes 5-7), and when dephosphorylation was triggered by addition of EGTA and excess ADP (to test for reversibility of the ATP phosphorylation reaction, lanes 8-10): in the latter case, too, most of the p95 fragment remained phosphorylated in an unusually stable state, although most of intact ATPase and p83C dephosphorylated within 5 seconds.

If interpreted within the framework of the four step-catalytic cycle generally used for intact Ca^{2+}-ATPase ($Ca_2E1 \rightarrow Ca_2E1P \rightarrow E2P \rightarrow E2$; see *Makinose, 1973*), this fact suggests that for p95C the processing of phosphoenzyme from its initial ADP-sensitive form to a subsequent ADP-insensitive form remains possible (the "Ca_2E1P to E2P" transition), but hydrolysis of the ADP-insensitive form is dramatically slowed down (the "E2P to E2" step), so that at steady-state a significant proportion of the latter phosphoenzyme form accumulates. Using previously established conditions (alkaline pH and no potassium) to directly measure the rate of the transition at which phosphoenzyme becomes insensitive to ADP, i.e. is converted from Ca_2E1P to E2P (e.g. *Vilsen et al., 1989)*, we were indeed able to confirm that the latter transition is reasonably fast in p95C peptide, as it is in intact ATPase *(see Fig 3bis in the Supplemental Data section).*

Phosphorylation from [^{32}P]Pi of the p95C/p14N complex is also, like dephosphorylation, much slower than for intact ATPase, and in equilibrium experiments this results in almost unaltered apparent affinity for Pi.

We then further studied the properties of the ADP-insensitive form of phosphoenzyme, after forming it from Pi via the "backdoor" reaction in the presence of 25 % DMSO (*de Meis et al., 1980*). Lanes 2 and 3 in *Fig 4* show that over a period of 1- 3 minutes at room temperature, the p95C peptide could become phosphorylated from Pi just as completely (or perhaps even to a slightly larger relative extent) than intact ATPase. Nevertheless, phosphorylation of the p83C peptide was a much less favourable (compare with Coomassie blue staining in Panel C) and also slower event, as previously demonstrated (*Møller et al., 2002)*. Ca^{2+}-independent phosphorylation from Pi in the presence of DMSO was also measured on ice (lanes 4-7 in *Fig 4*). In this case, phosphorylation of p95C again proved possible, up to quite high a final phosphorylation level, but at a rate that was much slower than for intact ATPase (whereas phosphorylation of p83C was very faint*).* After half an hour of phosphorylation under these conditions, dephosphorylation was triggered by a 10-fold dilution of the phosphorylated membranes into a DMSO-free, but KCl- and ATP-containing medium similar to that previously used to measure p95C dephosphorylation after ATP-dependent phosphorylation in *Fig 3*: although intact ATPase dephosphorylated very rapidly (as expected), this was not the case for p95C which dephosphorylated very slowly. This fully confirms that the slow dephosphorylation rate and reduced ADP-sensitivity inferred from the ATP phosphorylation experiment in Fig 3 are mainly due to a severe slowing down of the "E2P to E2" transition in the p95C/p14N complex. At 20°C, we again observed both a slowing down of the phosphorylation rate (from Pi) and a slowing down of the dephosphorylation rate of p95C (here, after addition of excess nonradioactive Pi in the continued presence of DMSO), compared with the corresponding rates of intact ATPase (see *Fig 4bis* in the Supplemental Data section).

Remarkably, when Pi-derived phosphorylation measurements were now performed *at equilibrium*, in the presence of increasing concentrations of Pi, the apparent affinities for Pi of p95C/p14N and intact ATPase proved similar (lanes 2-5 in *Fig 5*) (while phosphorylation was much less favourable for the p83C peptide (lanes 2-5 of *Fig 5)*, in accordance with our previous results in *Møller et al., 2002)*. As Pi-derived phosphorylation of ATPase is known to be Mg^{2+}-dependent (possibly because Mg.Pi is the real substrate, see *Champeil et al., 1985),* we also checked the effect of increasing concentrations of Mg^{2+} (see *Fig 5bis* in the Supplemental Data section) and again found no obvious difference in the apparent affinity of p95C/p14N and intact ATPase for Mg^{2+} concerning Pi-derived phosphorylation at equilibrium (however, p83C again did show such a difference, as expected). The similar apparent affinities found at equilibrium for p95C/p14N and for intact ATPase imply that phosphorylation and dephosphorylation rates are reduced by a similar factor in the complex, compared to the rates in intact ATPase. Thus, after ATPase cleavage at Leu^{119}-Lys^{120}, the Pi-derived phosphorylated form of the p95C/p14N complex is neither stabilized nor destabilized relative to the unphosphorylated form, but the kinetics of the phosphorylation/dephosphorylation reactions are slowed down, i.e. the energy barrier for the reaction is higher.

The unphosphorylated p95C/p14N complex has a poorer affinity for Ca^{2+} and a reduced rate of reaction with Ca^{2+}, compared with intact ATPase.

To investigate the Ca^{2+} binding properties of properties of the p95C/p14N complex, we measured the apparent competition, at equilibrium, between Ca^{2+} binding and phosphorylation from Pi. This is shown in lanes 5-9 of the preceding *Fig 5*. Despite the fact that such experiments only can give an apparent affinity for Ca^{2+}, as the efficiency of Ca^{2+} for preventing phosphorylation from Pi also depends on the equilibrium between phosphorylated and non-phosphorylated forms of Ca^{2+}-free ATPase, the results are quite clear. Firstly, a Ca^{2+} concentration of about 20 μM was required to inhibit phosphorylation from Pi of intact

ATPase by 85 %; the EC50 was about 6 µM, i.e. higher than the micromolar Ca½ for equilibrium binding of Ca^{2+} at pH 7 in the absence or presence of DMSO (e.g. *Champeil et al., 1985*), but such an apparent shift towards higher Ca^{2+} concentrations is consistent with the fact that in the presence of 200 µM Pi and DMSO, phosphorylation from Pi competes with Ca^{2+} binding to intact ATPase. Secondly, a Ca^{2+} concentration of only 2 µM (pCa 5.7) was sufficient to inhibit phosphorylation from Pi of the p83C peptide to a similar relative extent, in agreement with the above-mentioned unfavourable phosphorylation of this peptide from Pi and the unaltered true affinity of this peptide for Ca^{2+} (*Møller et al., 2002)*. Finally, phosphorylation of the p95C peptide was only reduced by half at 20 µM (pCa 4.7); since the p95C/p14N complex and intact ATPase are phosphorylated with roughly the same apparent affinity for Pi, the reduced efficiency of Ca^{2+} for preventing phosphorylation from Pi suggests a loss in affinity for Ca^{2+} in the p95C/p14N complex (see also *Fig 7* below for confirmation).

To learn more about the kinetics of the Ca^{2+}-dependent transition from E2 to Ca_2E1, we then turned back to Ca^{2+}-dependent phosphorylation from [γ-^{32}P]ATP; we repeated measurements, on ice, similar to those in *Fig 3*, except that before being added to the phosphorylation medium (which contained an excess of Ca^{2+} and [γ-^{32}P]ATP), PK-treated membranes were now left in the presence of EGTA in order to allow the Ca^{2+}-*free* fragments to react with Ca^{2+} and ATP at the same time (*Fig 6*). Phosphorylation of p95C was definitely slower under these conditions (compare with the results in lanes 2-4 in *Fig 3*), and much slower than phosphorylation of p83C or intact ATPase. This indicates that in p95C the calcium-induced transition from the Ca^{2+}-free form to the Ca^{2+}-bound and phosphorylatable form is relatively slow. The same fact was observable when experiments were repeated at 20 °C with the rapid mixing and quenching machine (see *Fig 6bis* in the Supplemental Data section).

This slow transition allowed us to design a protocol for estimating by a phosphorylation assay the "true" affinity of Ca^{2+} binding to p95C. In this experiment, PK-treated fragments were pre-equilibrated at various pCa values, and we measured the amount

of phosphorylated p95C after only 5s incubation with [γ-^{32}P]ATP, anticipating from the results in *Fig 6* that fragments of p95C phosphorylated after this period would correspond to those ATPase fragments which already had Ca^{2+} bound to them (since Ca^{2+}-free p95C fragments are unable to react with ATP within such a short period). *Fig 7* shows that the $Ca_{½}$ for EP formation by the p95C/p14N complex after only 5s was between 2 and 20 μM, i.e. higher than what is known from literature for intact SR or p83C under the same conditions (e.g. *Møller et al., 2002*) (and in fact also found in this experiment). This finding therefore confirms the above conclusion that the true affinity for Ca^{2+} of the p95C/p14N complex is slightly reduced, relative to that of intact ATPase. Note that when EP measurements are performed after 30 s phosphorylation instead of only 5 s, the difference between $Ca_{½}$ values for the p95C/p14N complex and intact ATPase is not as pronounced (see *Fig 2bis* in the Supplemental Data section), presumably because under that steady-state situation, the strong inhibition of dephosphorylation compensates for the true loss in calcium affinity (see, for instance, a related discussion about effects of steady-state conditions in *Andersen et al. 2001)*.

Note that the small shift of the equilibrium affinity for Ca^{2+} suggested by *Figs 7 & 5*, combined with the much more pronounced slowing down of the Ca^{2+}-induced transition shown in *Fig 6*, might suggest that the reverse events accompanying Ca^{2+} dissociation from the p95C/p14N complex are also slightly slowed down, although probably not to the same extent as the Ca^{2+}-induced transition.

The "true" affinity with which Ca^{2+}-free unphosphorylated p95C/p14N complex binds ortho-vanadate tightly is poorer than that of intact ATPase.

We concluded above that the kinetic and equilibrium characteristics of phosphorylation of the p95C/p14N complex suggested a higher energy barrier for phosphorylation of this complex from Pi. Such a relative destabilization of the transition state for the phosphorylation/dephosphorylation reactions was confirmed in experiments in which we measured the true affinity with which this ATPase fragment can bind orthovanadate,

whose binding is generally considered to provide an analog of the transition state formed during phosphorylation from Pi. Such experiments were already performed long ago with intact SR (*Medda and Hasselbach, 1983)*, and they have been recently adapted to characterize the transition state of mutated ATPases (*Toustrup-Jensen and Vilsen, 2003; Clausen and Andersen, 2003*). The rationale is to incubate the membranes with vanadate for an extended period of time, to attain equilibrium, and subsequently to phosphorylate the sample from ATP for a reasonably short period of time and thereby measure the amount of ATPase that has not reacted with vanadate. Care must be taken, on the one hand, to keep the phosphorylation reaction period short enough to mimimize dissociation of previously formed ATPase-vanadate complexes, and on the other, to make it long enough to ensure full phosphorylation of all vanadate-free ATPase fragments. The result of such experiments with PK-treated SR membranes is illustrated in Fig 8. After one hour incubation at 20°C, vanadate was found to bind to intact ATPase with the expected sub-micromolar affinity, but the apparent affinity of the p95C/p14N complex for vanadate was shifted to higher concentrations by more than one order of magnitude.

Note, with reference to the above considerations, that if the phosphorylation period was increased from 30 s to 120 s after preincubation with vanadate, the amount of phosphorylated p95C became larger, suggesting for vanadate bound to p95C/p14N a relatively fast rate of dissociation, which fits with poorer binding. Note also that p83C/p28N was completely unable to bind orthovanadate tightly, as previously found (*Møller et al., 2002)* and attributed at least in part to a deficient "E2" conformation.

DISCUSSION

Methodology

The present data demonstrate the usefulness of combining phosphorylation protocols with an appropriate gel electrophoretic separation technique, to study the partial reactions of various Ca^{2+}-ATPase proteolytic fragments, even when only small relative amounts of these fragments are formed along with other cleavage products. Such a combination might also prove useful for the study of other P-type ATPases. For one of the Ca^{2+}-ATPase complexes resulting from cleavage, p83C/p28N, formed after cleavage at Glu^{243}, the results we obtained with the present combination of techniques are in agreement with those that we had obtained by different techniques *(Møller et al. 2002;* see additional discussion about the p83C peptide in the Supplemental Data section). This gives us confidence about the reliability of the results obtained concerning the complex which will be more specifically discussed here, p95C/p14N, resulting from cleavage at Lys^{120}.

The main effects of cleavage at Lys^{120}

With the aid of this methodology we found that disruption of the link between the *A*-domain and the second transmembrane span by cleavage of the Leu^{119}-Lys^{120} peptide bond gives rise to a pronounced decrease in the ATPase activity of SERCA1a, yet with retention of the capacity for almost full phosphorylation from ATP and Pi. The detailed analysis of the properties of the resulting p95C/p14N complex indicates that the reaction rates associated with E2P dephosphorylation or formation of E2P from E2 and Pi are both reduced by at least two orders of magnitude, without appreciably affecting the equilibrium constant of the reaction. In comparison, the rate for the E2 → Ca_2E1 transition is reduced less strongly, while phosphorylation of Ca_2E1 from ATP and the subsequent Ca_2E1P → E2P transition are affected to an even lesser extent. This pattern differs significantly from the pattern found for the previously studied N-terminal proteinase K cleavage product, the p83C/p28N complex, in which the link between the *A*-domain and M3 (the third membrane span) has been disrupted

by excision of the short MAATE^{243} sequence *(Møller et al. 2002)*: in that case proteinase K cleavage primarily results in severe reduction of the Ca^{2+} translocating $Ca_2E1P \rightarrow E2P$ transition and impaired capability to form E2P from Pi in the absence of Ca^{2+}.

To facilitate discussion, *Fig 9* summarizes the effects on the various transition rates that we have observed in the present work to result from ATPase cleavage at either Leu^{119}-Lys^{120} or Thr^{242}-Glu^{243} (this work and Møller et al., 2002). This Figure should nevertheless be regarded as a crude summary only, as data obtained under different conditions have been pooled. As concerns the p83C/p28N complex, the reduced rates indicated for phosphorylation from Pi and dephosphorylation of E2P are also somewhat tentative; they are based on the results in *Fig 3 and Fig 4bis of the Supplemental Data section (see additional discussion in the Supplemental Data section).*

The A-domain, a phosphatase domain?

A few years ago, the mutation of some of the transmembrane residues critical for Ca^{2+}-binding was also found to result in reduced rates of E2P dephosphorylation (reviewed in *Andersen, 1995*). However, these mutants generally had apparent affinities for Pi higher than normal, and therefore, defective proton binding to the counter-transport sites was suspected to be responsible for their reduced rates of dephosphorylation. Subsequently, mutation of Arg198 in the *A*-domain was found to moderately reduce the rate of dephosphorylation *(Daiho et al., 1999),* and more recently, a dramatically reduced rate of E2P dephosphorylation was observed for many mutants of Val^{200} near the T2 site in the *A*-domain of Ca^{2+}-ATPase (*Kato et al., 2003*). This was also the case for a mutant of Glu^{183} in the conserved TGES sequence of the *A*-domain (*Andersen et al, personal communication*), and a closely related situation has been described to occur after mutation of Thr^{214} in the conserved TGES sequence of the *A*-domain of Na^+,K^+-ATPase, where a 5-fold reduction of the dephosphorylation rate was found for the Thr$^{214} \rightarrow$ Ala mutant (*Toustrup-Jensen and Vilsen, 2003*). Independently, it has been suggested for Na^+,K^+-ATPase (Goldshleger and Karlish

1999; Patchornik et al. 2000) and H^+,K^+-ATPase (Shin et al., 2001) that the same glutamate residue of the TGES motif in the *A*-domain may be interacting with the phosphorylation site *via* the Mg^{2+} residue bound to the phosphorylated Asp^{351} in the catalytic site; this conclusion was derived from cleavage experiments performed in the presence of peroxide and ferrous ion, with Fe.ATP presumably acting as a substitute for Mg.ATP in the catalytic site. Thus, it is likely that the *A*-domain in general, and the TGES motive in particular, play a specific role in acid/base catalyzed cleavage in E2P of the aspartylphosphate bond at Asp^{351} (an effect which may be enhanced if the cavity formed by the parts of the *P*-domain and *A*-domains which surround the catalytic site in the E2P state is fairly hydrophobic, see *de Meis et al., 1980*). Our present demonstration of a dramatic inhibition after cleavage at Lys^{120} of the link between M2 and the *A*-domain fits well into this picture of the role of the *A*-domain.

All these results revive a concept, elaborated earlier in connection with studies on H^+-ATPases, of the *A*-domain being a "phosphatase" domain, acting at a late step of the ATPase cycle *(Serrano 1988; Portillo and Serrano, 1988; Portillo et al., 1996),* while the *N*-domain would act as a "kinase" domain in an early step of the ATPase cycle. As discussed by *Toustrup-Jensen and Vilsen, 2003,* this would also fit with the demonstrated existence, in non-ATPase members of the HAD family, of catalytic residues *outside* the Rossman fold (corresponding to the ATPase *P*-domain), to assist the nucleophilic attack of water during dephosphorylation.

Structural implications of the effect of proteolysis

To sum up, our data on proteolyzed Ca^{2+}-ATPase, in accordance with other evidence, suggest that the ATPase A-domain is critically involved in the ion-transport-dependent dephosphorylation experienced by ATPase after phosphorylation by ATP. From a structural point of view, it seems clear that extensive rotation of the *A*-domain parallel to the membrane accompanies the ATPase transition from its Ca^{2+}-bound E1 conformation (PDB accession number 1EUL) to its Ca^{2+}-free conformations -either stabilized by TG (*Toyoshima and*

Nomura, 2002, PDB accession number 1IWO) or, for two-dimensional membrane crystals, in the additional presence of decavanadate (*Toyoshima et al., 2000; Danko et al., 2001a; Xu et al., 2002;* PDB accession numbers for the modeled structures: 1FQU and 1KJU); this rotation is probably an essential element for the interaction of the *A*-domain with the *P*-domain and concomitant positioning of the TGES sequence in the vicinity of the catalytic site. The ATPase segments linking the cytosolic *A*-domain to the transmembrane region and containing the proteinase K cleavage sites (Lys^{120} and Glu^{243}), S2 and S3, could conceivably play a strategic role in this rotation, as the 1IWO Ca^{2+}-free structure shows that after rotation these segments interact with helices P6 and P7 of the P-domain *(Fig 10)*.

Nevertheless, the fact that the p95C/p14N complex is capable of being phosphorylated from Pi, at a slow rate but with an unaltered apparent affinity for Pi, implies that E2 and E2P conformations with a rotated *A*-domain can still be formed after cleavage of S2. In fact, some of our results with the p95C/p14N complex (the decreased affinity for Ca^{2+}, the slower E2 to Ca_2E1 transition, and the accumulation of E2P during turnover) might even be interpreted as suggesting that both the E2 and E2P conformations are slightly stabilized in the proteolyzed complex (relative to the Ca^{2+}-bound conformation), as if cleavage at Lys^{120} does not prevent, but even favours stable reorientation of the *A*-domain (in contrast with cleavage at Glu^{243}, see *Møller et al., 2002*). Provided that *both* E2 and E2P are stabilized to the same extent, this would not be inconsistent with an unaltered affinity of equilibrium phosphorylation from Pi.

However, in continuation of the above considerations we still need to address the most remarkable effect of proteolytic cleavage of S2, i.e. the dramatic slowing down of the *rates* of phosphorylation from Pi and of dephosphorylation, an effect likely to reflect perturbation of the pathway through which *A*- and *P*-domains can change their mutual interactions during the enzymatic cycle. Of course, this perturbation may stem in part from entropic effects, as new conformations made available (at least locally) by the chain disruption may reduce the probability for proceeding along the normal reaction pathway. But in addition, as previously discussed in connection with similar effects observed for some mutants in this region

(*Andersen and Vilsen, 1993; Toustrup-Jensen and Vilsen, 2003),* the fact that in the p95C/p14N complex both forward and reverse rates of backdoor phosphorylation from Pi are apparently reduced to the same extent may imply relative destabilization of the transition state for the phosphorylation reaction. In support of this view we indeed observed a reduction in the affinity with which the p95C/p14N complex binds orthovanadate, a ligand which is considered as an analog of the pentacoordinated transition state of the phosphoryl group *(Cantley et al., 1978).*

It is difficult at present to discuss the structural basis for this observation, as we do not have any high resolution structure of this transition state at our disposal. However, by fitting the E1 high resolution 3-D structure into low density maps of two-dimensional membrane crystals, two models have been proposed for decavanadate-reacted Ca^{2+}-ATPase (Protein Data Bank accession codes 1FQU *(Toyoshima et al., 2000)* and 1KJU *(Xu et al. 2002))*, an ATPase form that probably also contains orthovanadate and may therefore provide the best presently available approximation of the transition state of the protein during dephosphorylation. In this ATPase form, both models suggest changes relative to the E2 form (1IWO), consisting in particular in a lifting up of the *A*-domain towards the *P*-domain, accompanied by a stretching of the S1-S3 segments. In 1FQU (*see Fig. 10bis in the Supplemental Data section*) it is somewhat disappointing that bonds shown to be present in the E2 form between S2 and the P-domain (namely the electrostatic interaction between Glu^{113} and Arg^{334} and the H-bond between Tyr^{122} and Val^{726}) are now broken and not replaced by new stabilizing bonds between S2 and the P-domain (instead, Glu^{113} and Glu^{123} reorient to form bonds with Arg^{47} and Leu^{41}, respectively, in the S1-loop); from this structure, it is not clear why proteolysis at Leu^{119}-Lys^{120} would prevent proper interaction of the *A*-domain and *P*-domains. On the other hand, in the 1KJU modeled structure, which is more compact than 1FQU and in which the TGES residues are placed in closer apposition to the phosphorylatable Asp^{351} residue, the flexible loops between the various domains have been rebuilt and energy-minimized *(Xu et al., 2002)*. In this model the resulting structure does

suggest the formation of many new bonds between S2 and the central part of the N-terminal structure, including residues in the immediate proximity of the proteolytic cleavage site (*Fig. 10bis in the Supplemental Data section*). Part of the explanation for the effect of cleavage at Lys120 may therefore indeed be that cleavage prevents formation of bonds essential for attaining the transition state.

Of course, future high resolution structures of 3D crystals of a transition-like state will be necessary to confirm or reject this possibility. At this step, however, the above possibility does not seem implausible, especially in view of very recent results concerning the Glu^{40}-Ser^{48} loop of the S1 segment (Daiho et al., 2003). In that work it was beautifully demonstrated that single deletion of any of the residues in that loop causes a dramatic slowing down of both the Ca_2E1P to E2P transition and the E2P to E2 transition, although simple mutation of the same residues had essentially no effect. This shows that the length of the S1 loop is critical for allowing the ATPase to reach its E2P state, as if formation of the catalytic site for optimal dephosphorylation or phosphorylation from Pi requires some further movement of the *A*-domain away from the membrane, as suggested in both the 1FQU and 1KJU modeled structures.

As indicated in Fig. 9, cleavage of Ca^{2+}-ATPase at Glu^{243} in the segment linking the *A*-domain and S3 gives rise to a different phenotype for the resulting p83C/p28N complex, where the Ca_2E1P to E2P transition and the E2P dephosphorylation are both strongly inhibited. In the case of this complex, we could measure inhibition of Ca^{2+} transport, too (*Møller et al., 2002)*, while in the case of the p95C/p14N complex, we have no evidence at present that disruption of the S2 segment has any effect on translocation, beyond the expected slowing down of activity. However, it remains a tempting idea that in addition to locally changing the A/P interactions, disruption of the loops between the *A*-domain and the transmembrane region prevents mechanical forces to be transmitted from the catalytic domains to the transport sites and vice-versa, especially perhaps via the S3 and S1 links. If movement of the *A*-domain (parallel and perpendicular to the membrane plane) leads to both

phosphoenzyme hydrolysis and ion transport, this could also justify revival of the old name of "transduction domain" that was once given to the *A*-domain, although on the basis of controversial experiments (Scott & Shamoo, 1982; Torok et al., 1988; Shoshan-Barmatz et al., 1987). The segments which have been proteolyzed in the present work could be among the controlling elements which coordinate events at the cytosolic catalytic site with events at the membranous transport sites, as requested by the "coupling rules" of active transport *(Jencks, 1989)*.

Acknowledgments

We thank Pr Robin Post for suggesting us to try and measure the effect of cleaving the ATPase at Leu^{119}-Lys^{120}, as well as for helpful comments on our draft. We also thank J. P. Andersen & J.D. Clausen for communicating to us the results of their unpublished experiments with ATPase mutants and for extensive discussion, as well as for tips on how to make EP measurements more reproducible, Bitten Holm for her assistance in some of these experiments, Paulette Decottignies-Le Maréchal (Université Paris XI, Orsay) for her help with N-terminal sequencing, Chikashi Toyoshima for discussion, the Human Frontier Science Program Organization for support (RGP 0060/2001-M), and the Ministère Français de la Recherche for financial support of G.L.

REFERENCES *(References will be given numbers in the final revised version)*

Møller, J. V., Lenoir, G., Marchand, C., Montigny, C., le Maire, M., Toyoshima, C., Juul, B. S., and Champeil, P. (2002) *J. Biol . Chem.* **277**, 38647-38659.

Møller, J. V., Lenoir, G., le Maire, M., Juul, B. S., and Champeil, P. (2003) A*nn. N.Y. Acad. Sci.* ***986,*** 82-89.

Juul, B., Turc, H., Durand, M.L., Gomez de Gracia, A., Denoroy, L., Møller, J.V., Champeil, P. and le Maire, M. (1995) *J Biol. Chem.* **270**, 20123-20134.

Champeil, P., Guillain, F., Vénien, C. and Gingold, M. P. (1985) *Biochemistry* **24**, 69-81.

Sarkadi, B., Enyedi, A., Földes-Papp, Z., Gárdos, G. (1986) *J. Biol. Chem.* **261,** 9552-9557.

Sarkadi, B., Enyedi, A., Penniston, J. T., Verma, A. K., Dux, L., Molnár, E. and Gárdos, G. (1988) *Biochim. Biophys. Acta* **939***, 40-46*.

Echarte, M. M., Levi, V., Villamil, A. M., Rossi, R. C. and Rossi, J. P. (2001) *Anal. Biochem.* **289**, 267-273.

Tsivkovskii, R ., Eisses, J. F., Kaplan, J. H., and Lutsenko, S. (2002) *J. Biol. Chem.* **277**, 976-983.

Shevchenko, A., Wilm, M., Vorm, O., and Mann, M. (1996) *Anal. Chem.* **68**, 850-858.

Guex, N. and Peitsch, M.C. (1997) *Electrophoresis* **18**, 2714-2723.

Tong, S. W. (1977) *Biochem. Biophys. Res. Comm.* **74**, 1242-1248.

Menguy, T., Corre, F., Bouneau, L., Deschamps, S., Møller, J.V., Champeil, P., le Maire, M. and Falson, P. (1998) *J. Biol. Chem.* **273**, 20134-20143.

Makinose, M. (1973) *FEBS Lett* **37**, 140-143.

Soulié, S., Møller, J.V., Falson, P. and le Maire, M. (1996) *Anal. Biochem.* **236**, 363-364.

Champeil, P., Menguy, T., Soulié, S., Juul, B., Gomez de Gracia, A., Rusconi, F., Falson, P., Denoroy, L., Henao, F., le Maire, M. and Møller, J. V. (1998) *J. Biol. Chem.* **273**, 6619-6631.

Champeil, P., Menguy, T., Tribet, C., Popot, J. L. and le Maire, M. (2000) *J. Biol. Chem.* **275**, 18623-18637.

Danko, S., Daiho, T., Yamasaki, K., Kamidochi, M., Suzuki, H. and Toyoshima, C. (2001a) *FEBS Lett*. **489**, 277-282.

Danko, S., Yamasaki, K., Daiho, T., Suzuki, H. and Toyoshima, C. (2001b) *FEBS Lett.* **505**, 129-135.

Ma, H., Inesi, G. and Toyoshima, C. (2003) *J. Biol. Chem.* **278**, 28938-28943.

Toyoshima, C., Nakasako, M., Nomura, H. and Ogawa, H. (2000) *Nature* **405**, 633-634.

Toyoshima, C., and Nomura, H. (2002) *Nature* **418**, 605-611.

Pick, U. and Karlish, S. J. (1982*) J. Biol. Chem.* **257**, 6120-6126

de Meis, L., Martins, O. B. and Alves, E. W. (1980) *Biochemistry* **19**, 4252-4261.

Clarke, D. M., Loo, T. W., Inesi, G., and MacLennan, D. H. (1989) *Nature* **339**, 476-478.

Andersen, J.P., and Vilsen, B. (1992) *J. Biol. Chem.* **267**, 19383-19387.

Sørensen, T. L., Vilsen, B., and Andersen, J. P. (1997) *J. Biol. Chem.* **272**, 30244-30253.

Andersen, J. P., Sørensen, T. L., Povlsen, K., and Vilsen, B. (2001) *J. Biol. Chem.* **276**, 23312-23321.

Kato, S., Kamidochi, M., Daiho, T., Yamasaki, K., Gouli, W., and Suzuki, H. (2003) *J. Biol. Chem.* **278**, 9624-9629.

Toustrup-Jensen, M., and Vilsen, B. (2003) *J. Biol. Chem.* **278**, 11402-11410.

Daiho, T. Suzuki, H., Yamasaki, K., Saino, T., and Kanazawa, T. (1999) *FEBS Lett* **444**, 54-58.

Andersen, J. P. (1995) *Biosciences Reports* **15**, 243-261.

Andersen, J. P., and Vilsen, B. (1993) *Biochemistry* **32**, 10015-10020.

Goldshleger, R., and Karlish, S. J. D. (1999) *J. Biol. Chem.* **274**, 16213-16221.

Patchornik, G., Goldshleger, R., and Karlish, S. J. D. (2000) *Proc. Natl. Acad. Sci. US* **97**, 11954-11959.

Shin, J. M., Goldshleger, R., Munson, K. B., Sachs, G., and Karlish, S. J. D. (2001) *J. Biol. Chem.* **276**, 48440-48450.

Serrano, R. (1988) *Biochim. Biophys. Acta* **947**, 1-28.

Portillo, F., and Serrano, R. (1988) *EMBO J.* **7***,* 1793-1798.

Portillo, F., Eraso, P., and Serrano, R. (1996) *in Biomembranes, ATPases, Vol. 5 (Lee, A.G., ed.) JAI Press, Greenwich),* pp225-240.

Cantley, L. C., Jr., Cantley, L. G., and Josephson, L. (1978) *J. Biol. Chem.* **253**, 7361-7368

MacLennan, D. H., Clarke, D. M., Loo, T. W., and Skerjanc, I. S. (1992), *Acta Physiologica Scandinavica* **146**, 141-150.

Vilsen, B., Andersen, J. P., Clarke, D. M., and MacLennan, D. H. (1989) *J. Biol. Chem.* **264**, 21024-21030.

Medda, P., and Hasselbach, W. (1983) *Eur. J. Biochem.* **137**, 7-14.

Toustrup-Jensen, M, and Vilsen, B. (2003) *J. Biol. Chem.* **278**, 11402-1410.

Clausen, J. D., and Andersen, J. P. (2003) *Biochemistry* **42**, 2585-2594.

Andersen, J. P., and Vilsen B. (1993) *Biochemistry* **32**, 10015-10020.

Daiho, T., Yamasaki, K., Wang, G., Danko, S., Iizuka, H., and Suzuki, H. (2003) *J. Biol. Chem., in press*.

Scott, T.L. and Shamoo, A.E. (1982) *J Membr Biol* **64**, 137-144.

Torok, K., Trinnaman, B.J. and Green, N. M. (1988) *Eur J Biochem* **173**, 361-367.

Shoshan-Barmatz V., Ouziel, N. and Chipman, D.M. (1987) *J Biol Chem* **262**, 11559-11564.

Xu, C., Rice, W. J., He, W., and Stokes, D. L. (2002) *J. Mol. Biol.* **316**, 201-211.

Jencks, W. P. (1989) *J. Biol. Chem.* **264**, 18855-18858.

FIGURE LEGENDS

Figure 1. Proteinase K (PK) treatment in the absence of Ca^{2+} results in cleavage at Leu^{119}-Lys^{120} and formation of a p95C/p14N complex (together with other peptides).

Sarcoplasmic reticulum (SR) membranes (2 mg protein/ml) were treated with PK (0.03 mg/ml) at 20°C in proteolysis buffer (100 mM Mops-NaOH, 5 mM Mg^{2+}, pH 6.5), in the presence of 0.3 mM Ca^{2+} (lanes 2-5) or the presence of 0.5 mM EGTA (lanes 6-9). Here, after proteolysis arrest aliquots of the various samples were added to an urea-containing denaturation buffer (essentially as described in *Soulié et al 1996*), boiled, and loaded (about 4 µg protein per lane) onto a 12 % SDS-PAGE Laemmli gel prepared in the presence of 1 mM Ca^{2+}. After Coomassie Blue staining, the intensity of individual peptide bands was deduced from gel scanning (Molecular Analyst). Lanes 1 and 10 contain molecular mass markers ("LMW" Pharmacia kit). The central part of the Figure schematises the identified points of primary cleavage and the various proteolytic products. The bottom part of the Figure shows an experiment in which the samples that were loaded onto the gel (with or without preliminary PK treatment, lanes 2 & 3 (two different samples) or lane 1, respectively) had first been solubilized and submitted to size exclusion chromatography in the presence of detergent, and had eluted at the position where monomeric uncleaved ATPase elutes. After SDS-PAGE separation, the gel was blotted onto an Immobilon membrane, and before staining with Coomassie blue the blot was immuno-revealed with an antibody specific for the ATPase N-terminus (see Methods).

Figure 2. Phosphorylation from [γ-^{32}P]ATP of the p95C/p14N complex, pre-equilibrated in the presence of Ca^{2+}, is only 3-fold slower than that of intact ATPase.

PK-treated membranes, initially at 0.4 mg/ml protein in buffer A supplemented with 150 µM Ca^{2+} and 100 µM EGTA, were mixed vol/vol with a medium containing 10 µM [γ–^{32}P]ATP and again 150 µM Ca^{2+} and 100 µM EGTA, and acid-quenched after various

periods at 20°C (except for the last lane, which is a duplicate of the previous one) in a rapid mixing-and-quenching equipment (hence the millisecond time scale) before SDS-PAGE separation of the various ATPase fragments. Lane 1 contained molecular mass markers ("PSMW", BioRad). Panel A shows the PhosphorImager scan. From this scan and from the Coomassie Blue staining ability of the various bands (Panel C), we computed the relative ability of the various bands to retain ^{32}P (as the ratio of ^{32}P radioactivity to Coomassie Blue staining), taking the maximal phosphorylation level of intact ATPase (at 200 ms) as 100 %. The actual amount of ^{32}P associated with the phosphorylated intact ATPase band at steady state was of the order of 2 pmol.

Figure 3. After steady-state phosphorylation from [γ-^{32}P]ATP, the p95C/p14N complex dephosphorylates very slowly, even in the presence of ADP.

PK-treated membranes were, after proteolysis arrest, supplemented with 0.55 mM Ca^{2+}, and phosphorylation was then triggered by diluting these membranes to 0.2 mg/ml protein into a phosphorylation medium, on ice, consisting of buffer A supplemented with 5 μM [γ–^{32}P]ATP, 100 μM Ca^{2+} and 50 μM EGTA. Membranes were phosphorylated for 5, 15 or 30 s (lanes 2-4). After phosphorylation for 30 s, dephosphorylation of the various fragments was either triggered by addition of 2 mM EGTA, 2 mM MgATP, 1 mM PEP and 0.02 mg/ml pyruvate kinase (to remove ADP as much as possible) and monitored after 5, 30 or 60 s (lanes 5-7), or triggered by addition of EGTA together with 1 mM ADP and again monitored after 5, 30, or 10 s (by mistake) (lanes 8-10). Lane 1 contained prestained molecular weight markers (PSMW). Panel A shows the PhosphorImager scan. From this scan and from the Coomassie Blue staining ability of the various bands (Panel C), we computed the relative ability of the various bands to retain ^{32}P (Panel B), taking the phosphorylation level of intact ATPase at 30 s as 100 %.

Figure 4. Backdoor phosphorylation from [^{32}P]Pi of the p95C/p14N complex is slowed down compared with intact ATPase, and dephosphorylation on ice in the presence of KCl is also slowed down.

PK-treated and resuspended membranes were reacted with 200 μM [^{32}P]Pi in buffer B supplemented with 25 % DMSO and 1 mM EGTA (lanes 2-5), and the kinetics of phosphorylation of the various bands was measured, both at 20°C (lanes 2-3, closed symbols in panel B) and on ice (lanes 4-7, open symbols in Panel B). After 30 min phosphorylation on ice, dephosphorylation was triggered by 10-fold dilution into DMSO-free buffer A, supplemented with 2 mM MgATP and 1 mM EGTA (similar results were obtained if excess non-radioactive Pi was also present, data not shown). Lane 1 contained molecular mass markers (LMW). Panel A shows the PhosphorImager scan. From this scan and from the Coomassie Blue staining ability of the various bands (Panel C), we computed the relative ability of the various bands to retain ^{32}P (Panel B), taking the phosphorylation level of intact ATPase after 3 minutes at 20°C as 100 %.

Figure 5. Phosphorylation from [^{32}P]Pi of the p95C/p14N complex occurs with quasi-normal affinity for Pi, and inhibition by Ca^{2+} is slightly less pronounced.

PK-treated and resuspended membranes were incubated for 15 minutes in buffer B supplemented with 25 % DMSO and either 1 mM EGTA and various concentrations of [^{32}P]Pi (lanes 2-5), or 200 μM [^{32}P]Pi and various concentrations of free Ca^{2+} (resulting in the pCa indicated, lanes 5-9). Lanes 1 and 10 contained molecular mass markers (LMW). Panel A shows the PhosphorImager scan. From this scan and from the Coomassie Blue staining ability of the various bands (Panel C), we computed the relative ability of the various bands to retain ^{32}P (Panel B), taking the phosphorylation level of intact ATPase at pCa 8.7 and 200 μM Pi as 100 %.

Figure 6. Phosphorylation from [γ-^{32}P]ATP of the p95C/p14N complex is slow when the complex initially is in a Ca^{2+}-deprived state, suggesting a slow E2 to Ca_2E1 transition.

Here, in contrast with the experiments illustrated in *Fig 3*, PK-treated membranes were left in EGTA (0.5 mM) after proteolysis arrest, and phosphorylation was triggered by 10-fold dilution of these membranes into a [γ-^{32}P]ATP-containing phosphorylation medium that had been supplemented with 100 μM Ca^{2+}. Phosphorylation was measured after various periods (lanes 2-4). Dephosphorylation after 30 s phosphorylation was also measured in the same experiment (lanes 5-7), but that is a mere repetition of the dephosphorylation experiment previously illustrated in lanes 5-7 of *Fig 3*, with similar results. Lanes 1 and 8 contained molecular mass markers (LMW and PSMW, respectively). Panel A shows the PhosphorImager scan. From this scan and from the Coomassie Blue staining ability of the various bands (Panel C), we computed the relative ability of the various bands to retain ^{32}P (Panel B), taking the phosphorylation level of intact ATPase at 30 s as 100 %. Circles: intact ATPase; squares, p95C peptide; triangles, p83C peptide.

Figure 7. The « true » affinity for Ca^{2+} binding indeed is slightly poorer for p95C than for intact ATPase.

Lanes 2-4 are a repetition of lanes 2-4 in the previous *Fig 6*, in which Ca^{2+}-free PK-SR was reacted with 50 μM free Ca^{2+} and 5 μM [γ–^{32}P]ATP simultaneously. Lanes 5-9 correspond to phosphorylation measurements where PK-treated membranes were first incubated at various pCa values, and phosphorylation from [γ–^{32}P]ATP at this pCa value was measured after 5 s reaction only. Lane 1 contained molecular mass markers (LMW). Panel A shows the PhosphorImager scan. From this scan and from the Coomassie Blue staining ability of the various bands (Panel C), we computed the relative ability of the various bands to retain ^{32}P (Panel B), taking the phosphorylation level of intact ATPase at 30 s as 100 %.

Figure 8. The "true" affinity with which Ca^{2+}-free unphosphorylated p95C/p14N

complex binds ortho-vanadate is clearly poorer than that of intact ATPase.

PK-treated membranes were diluted to 0.1 mg/ml protein in buffer A (100 mM KCl, 5 mM Mg^{2+} and 50 mM Mops/Tris at pH 7.0) supplemented with 0.2 mM EGTA, and incubated for 65 min at 20°C with various concentrations of ortho-vanadate. Samples were subsequently cooled on ice for 10 minutes, and phosphorylation was triggered by the simultaneous addition of 5 μM [γ-^{32}P]ATP and 300 μM Ca^{2+}. Acid quenching was generally performed after 30 s phosphorylation (120 s in the sample indicated by an asterisk, lane 10). Panel A shows the PhosphorImager scan. From this scan and from the Coomassie Blue staining ability of the various bands (Panel C), we computed the relative ability of the various bands to retain ^{32}P (as in Fig 2B), taking the maximal phosphorylation level of the intact ATPase band (in the absence of vanadate, lane 1) as 100 % (Panel B).

Figure 9. Summary of the functional effects of ATPase cleavage at either L^{119}-K^{120} or T^{242}-E^{243}.

Numbers given here are only very tentative figures, obtained by pooling for each transition the numbers obtained under different experimental conditions (temperature, DMSO, …).

Figure 10. Interface between A-and P-domains (S2/S3 and P6/P7) in the Ca^{2+}-free form of Ca^{2+}-ATPase.

This cartoon is based on the structure whose Protein Data bank accession code is 1IWO (including indications therein concerning the limits of the various secondary structures). In this structure, the top portions of S2 and S3 (dark blue and light blue, respectively) are facing the P7 and P6 helices, respectively (the latter helices are colored yellow); P6 is the helix at the beginning of which Asp^{707}, one of the residues conserved in all members of the whole HAD family, sits. In addition to the S2/S3-P6/P7 interface (amino-acids 111-124 are colored dark blue, and 230-247 are colored light blue), residues of special

interest are also indicated, especially conserved ones. Note that mutation of Gly^{233} and cleavage at Glu^{231} (references in *Møller et al. 2002*), on S3 at the same level as the top of P6, as well as mutation of Asn^{111} (see *MacLennan et al., 1992*), below Lys^{120} on S2, are critical for ATPase function.

Fig 1: Proteinase K (PK) treatment in the absence of Ca^{2+} results in cleavage at L119-K120 and formation of a p95C/p14N complex.

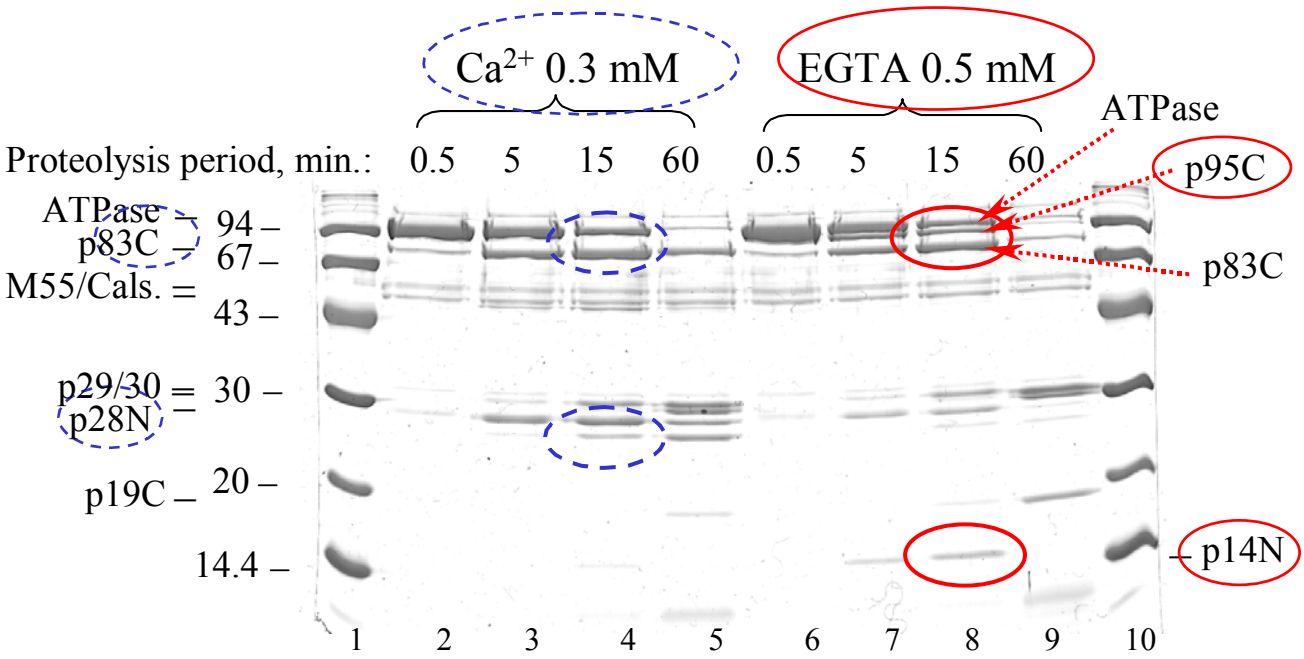

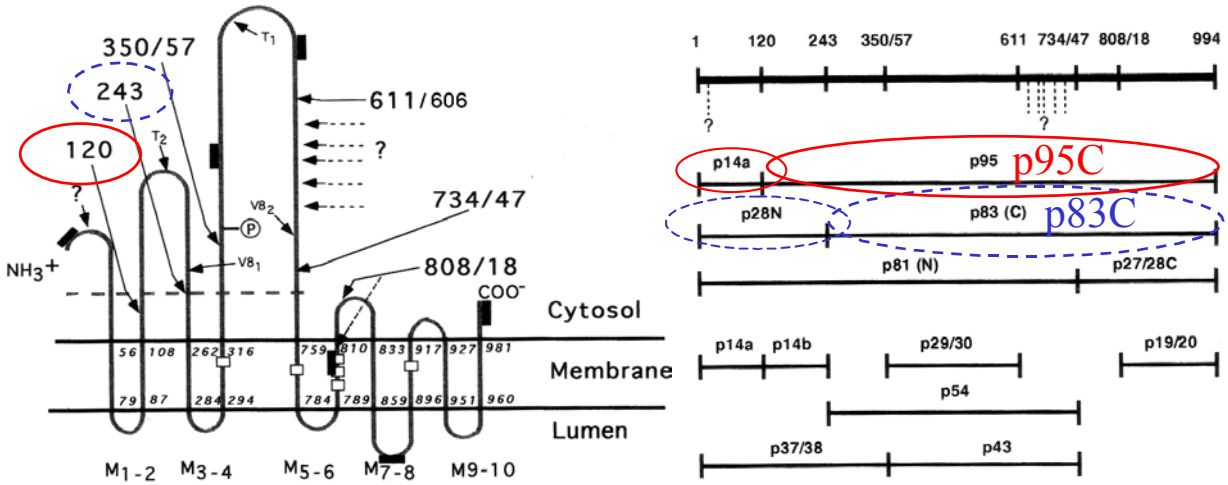

PK treatment before solubilization, HPLC and *analysis of eluted monomer fraction*:

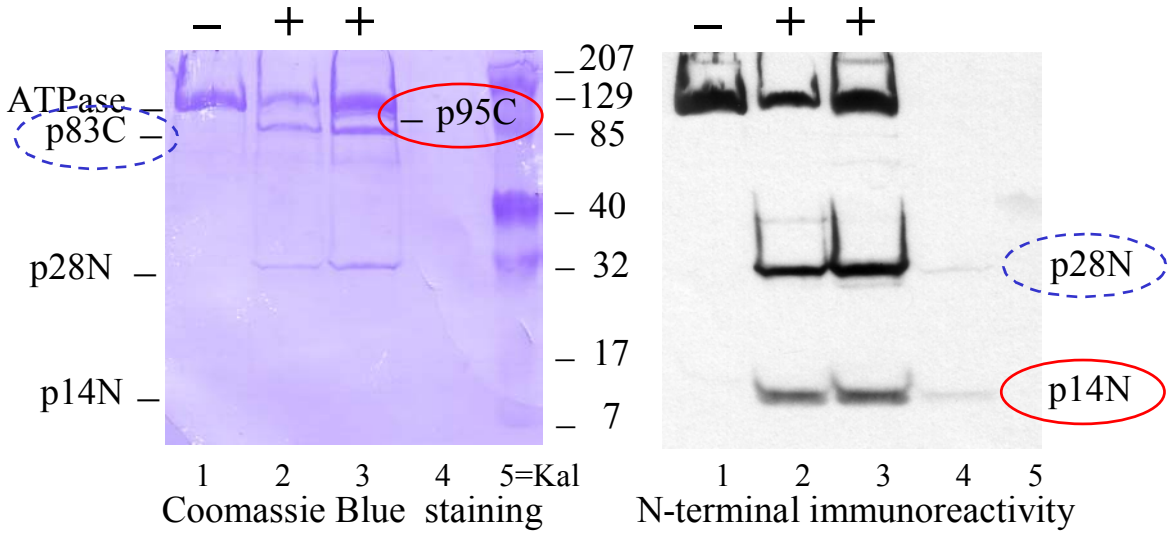

Fig 2. Phosphorylation from [γ-^{32}P]ATP of p95C/p14N, following pre-equilibration with Ca^{2+}, is only slightly slower than that of intact ATPase or p83C/p28N.

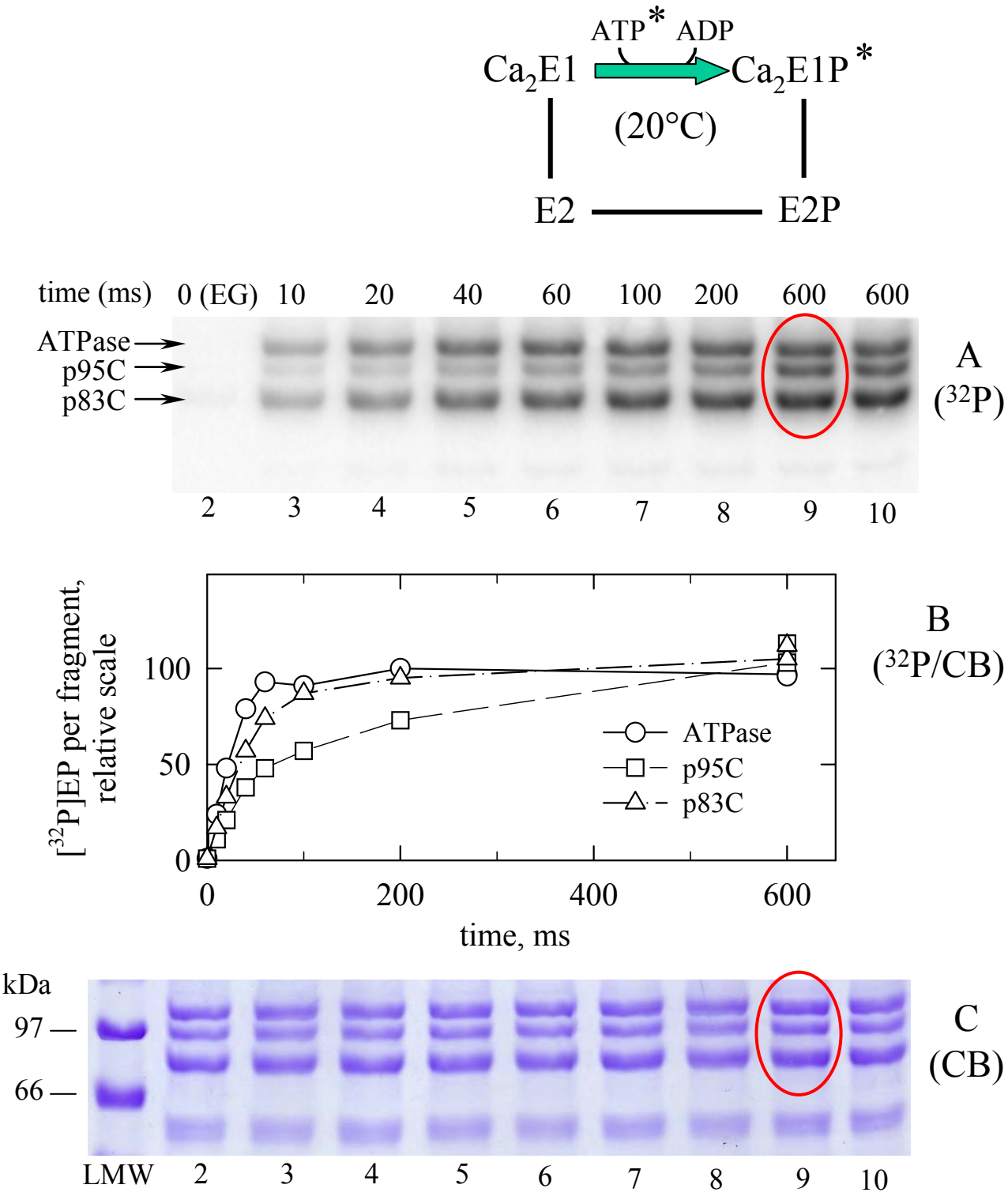

Fig 02_v4=QFM(Ca)_030507

Fig 3. After steady-state phosphorylation from [γ-^{32}P]ATP, p95C/p14N dephosphorylates very slowly, even in the presence of ADP.

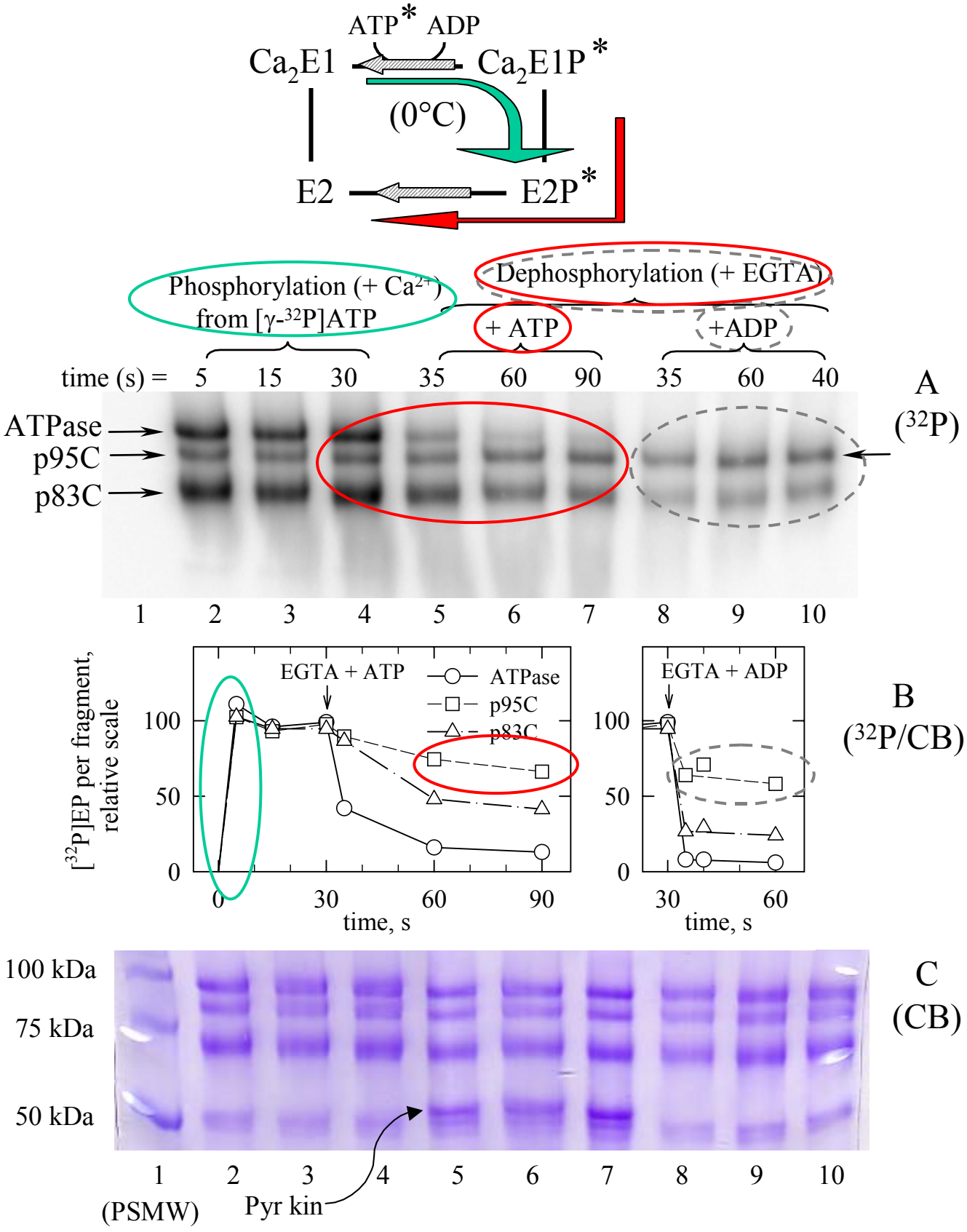

Fig 03_v4=p95 DEphosphorylation from ATP+/-ADP.ppt (+011024_c.jnb)

Fig 4. Backdoor phosphorylation from [^{32}P]Pi of the p95C/p14N complex is slowed down compared with intact ATPase, and dephosphorylation on ice in the presence of KCl is also slowed down.

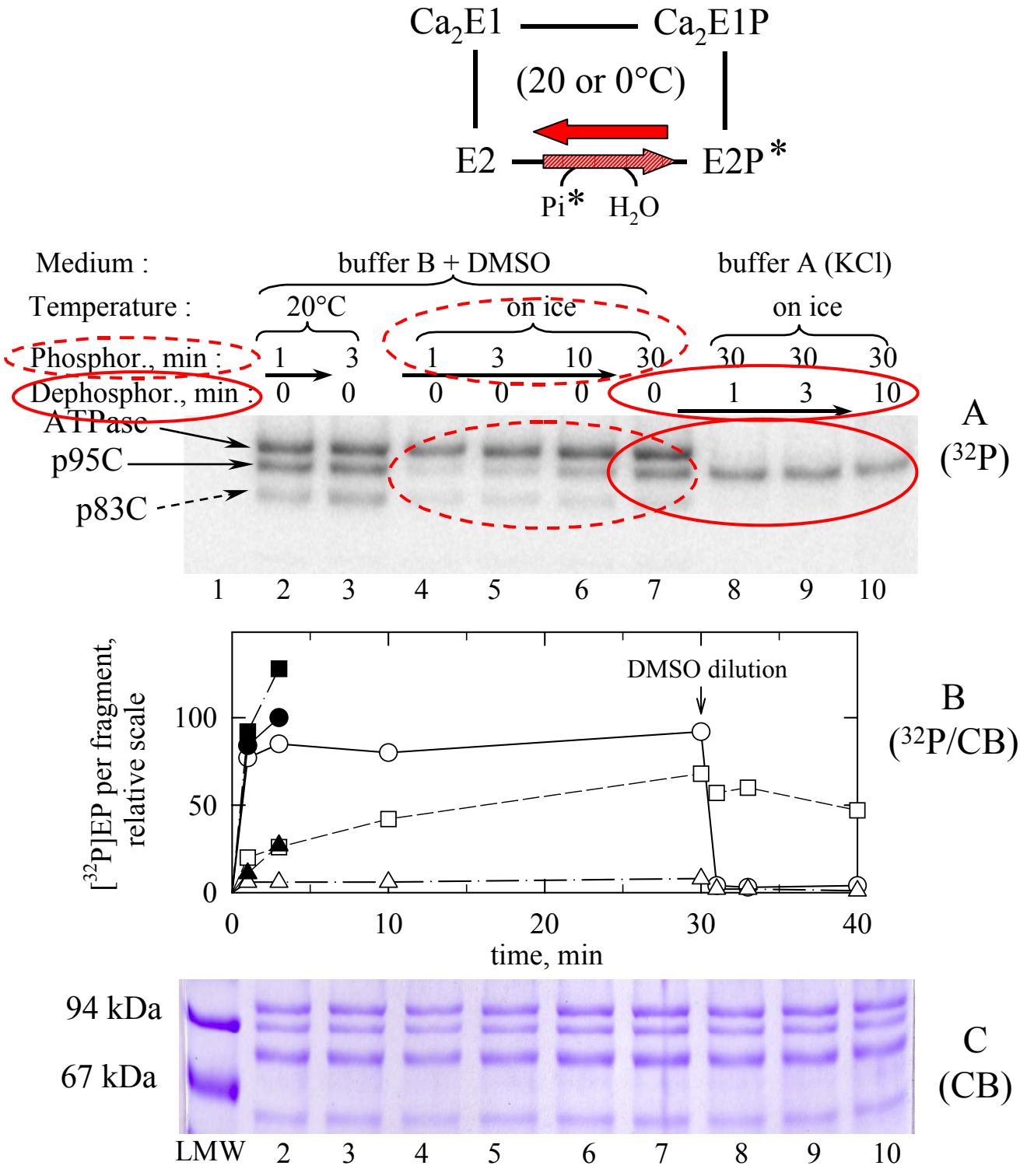

Fig 04_v4=kinetics of E2P dephosphorylation in KCl on ice (and phosphor)_030402a.ppt

Fig 5. Equilibrium phosphorylation from [^{32}P]Pi of the p95C peptide occurs with quasi-normal affinity for Pi.
Inhibition by Ca^{2+} is slightly less pronounced.

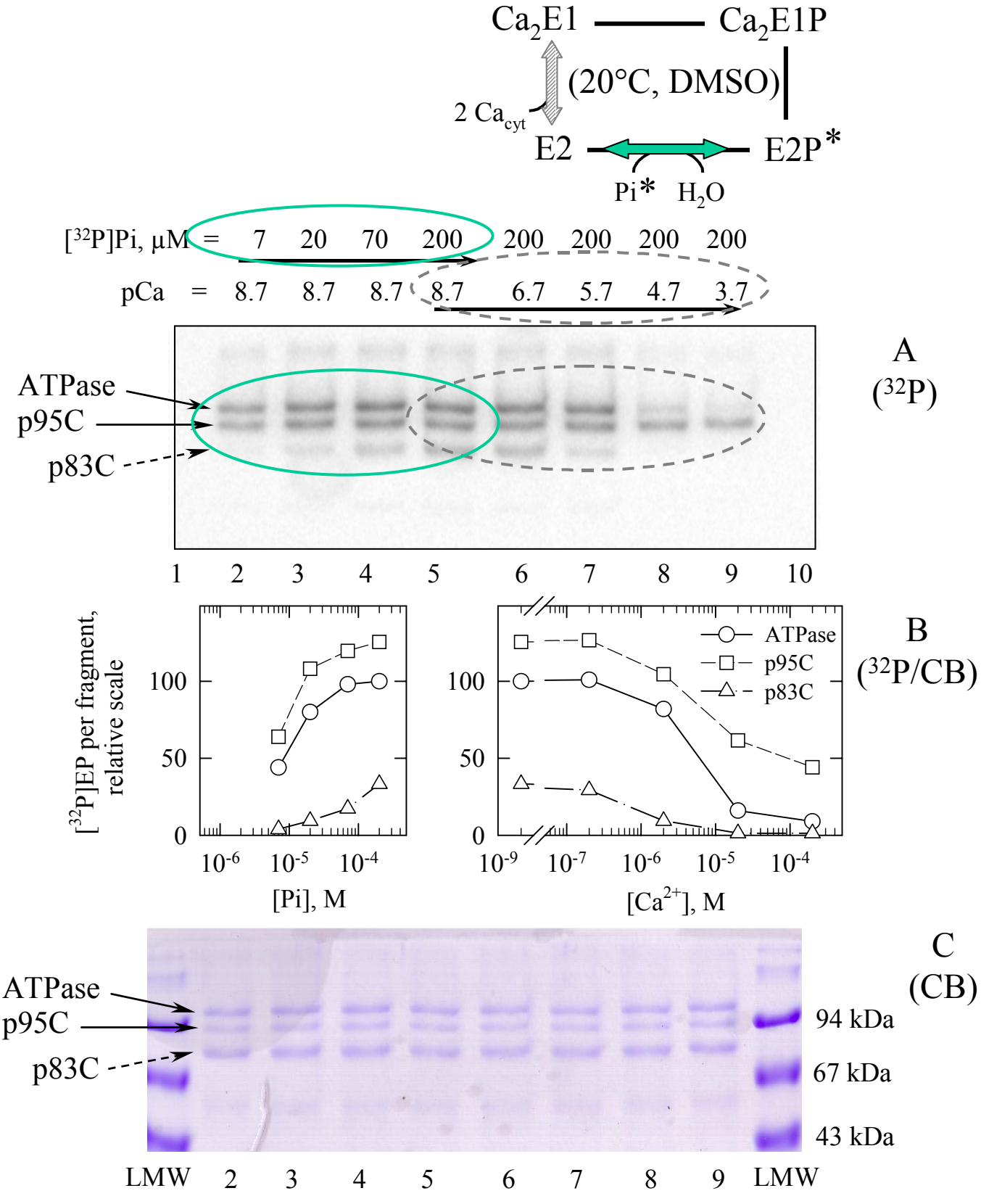

Fig 05_v4=E2P from Pi_030313 ac+ap.ppt (gris de ap accentués 2x); (+ 030313_a.jnb)

Fig 6. Phosphorylation from [^{32}P]ATP of the p95C/p14N complex is slow when the complex initially is in a Ca^{2+}-deprived state, suggesting a slow E2 to Ca_2E1 transition in p95C/p14N.

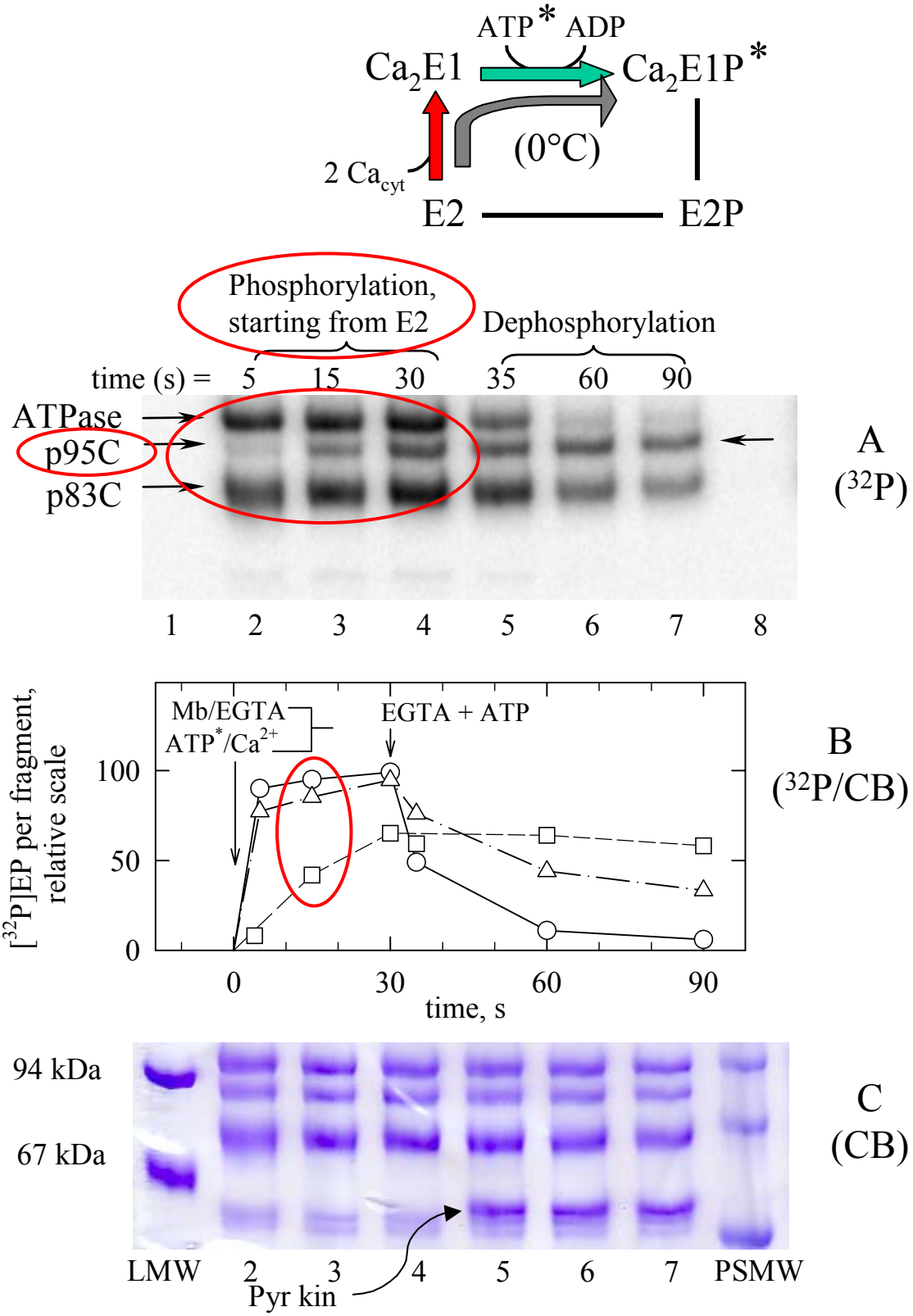

Fig 06_v4=p95 E2 to E1 transition, with ATP.ppt (011003)

Fig 7. The « true » affinity for Ca^{2+} binding indeed is slightly poorer for p95C than for intact ATPase.

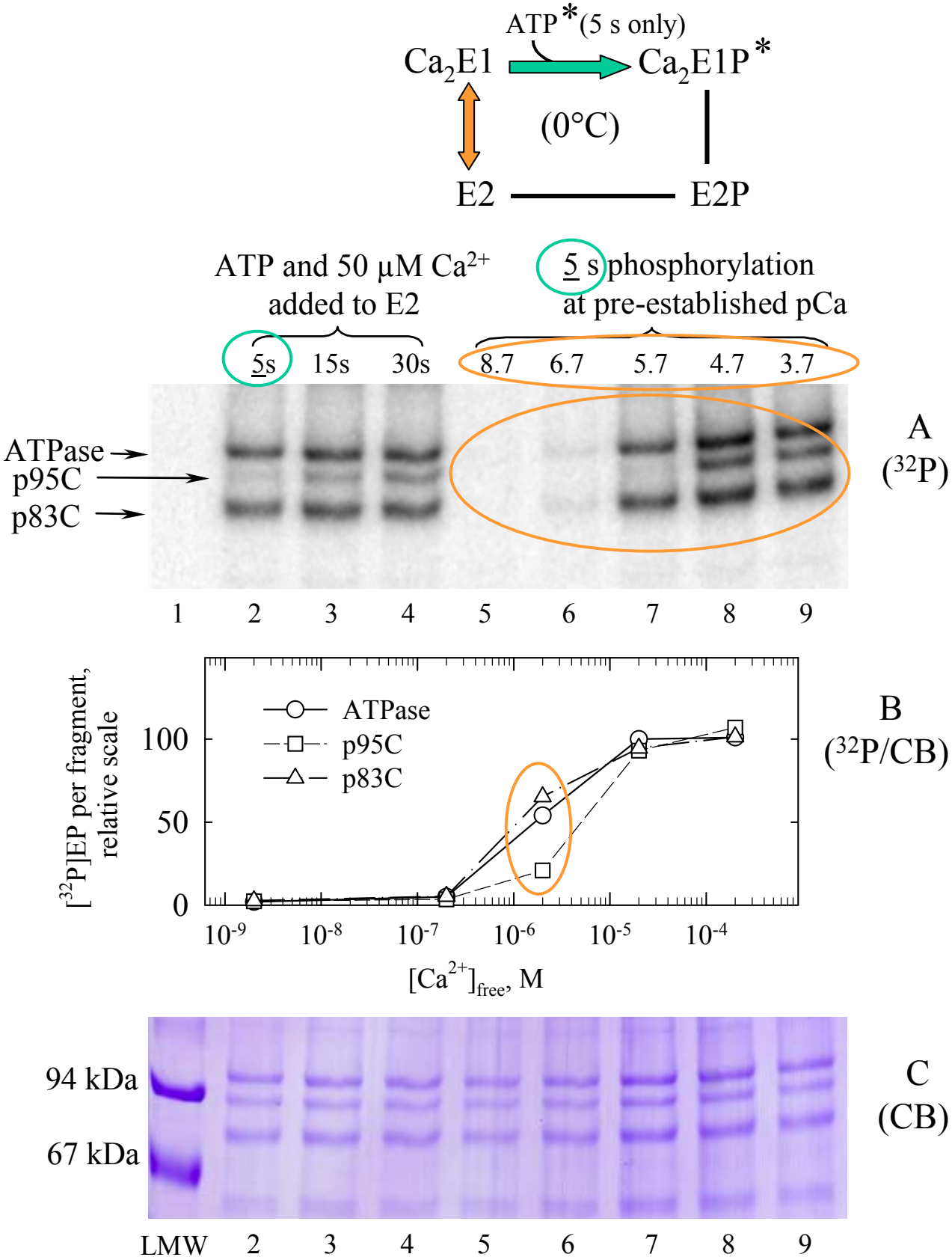

Fig 07_v4=p95 true affinity for Ca, from EP ATP_030318D.ppt

Fig 8. The « true » affinity with which Ca^{2+}-free p95C/p14N binds ortho-vanadate is clearly poorer than that of intact ATPase.

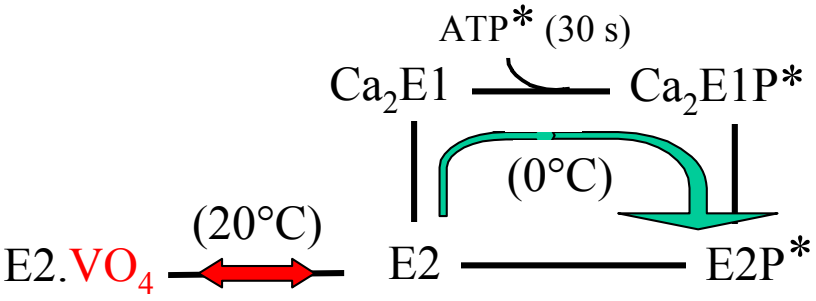

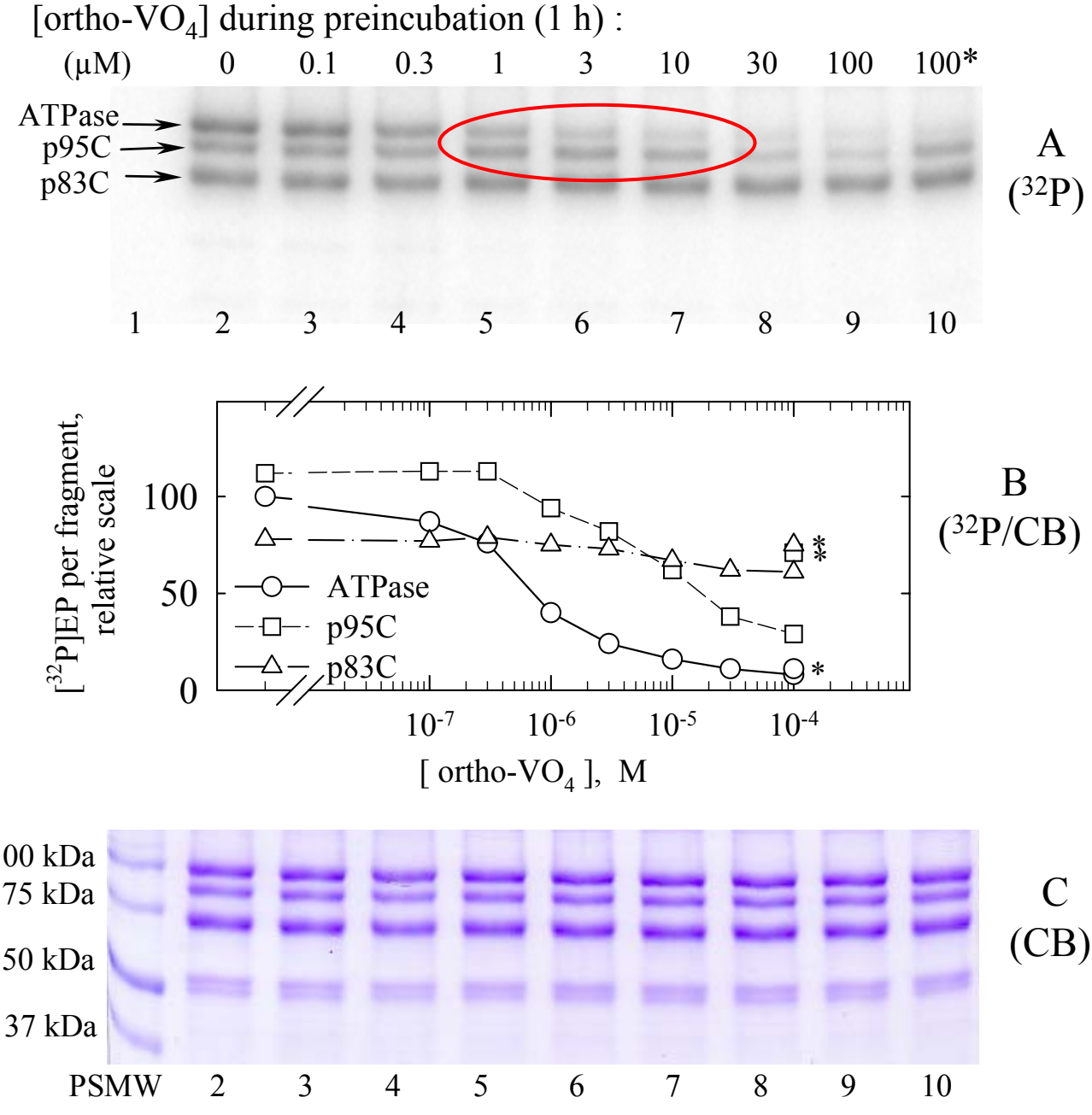

Fig 08_v4=p95 true affinity for VO4, from EP ATP_030612_c.ppt

Fig 9. Functional effects of cleavage close to the *A*-domain :

p95C/p14N versus intact ATPase :

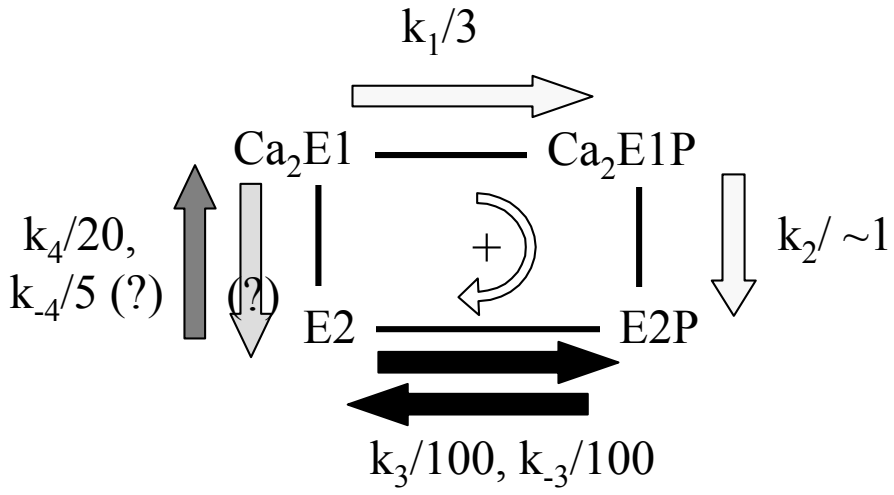

p83C/p28N versus intact ATPase :

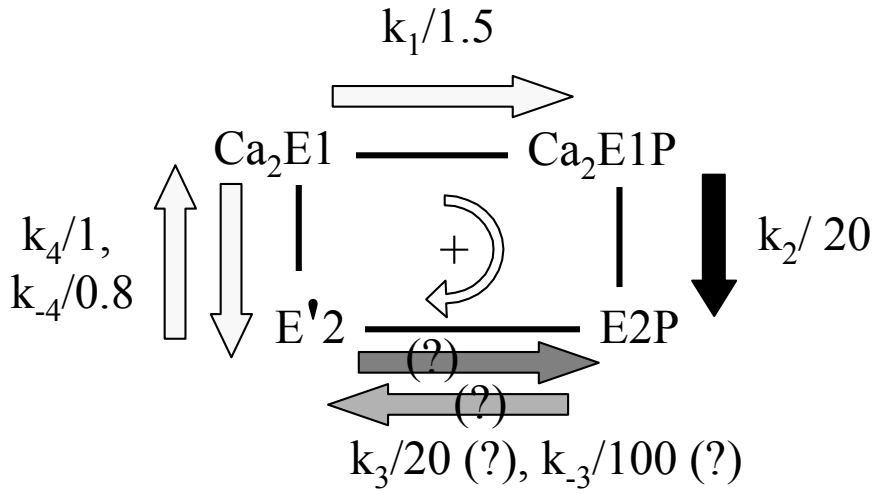

Fig 10. Interface between S2/S3 and P7/P6 in E2(TG) *(1IWO_PDB)*

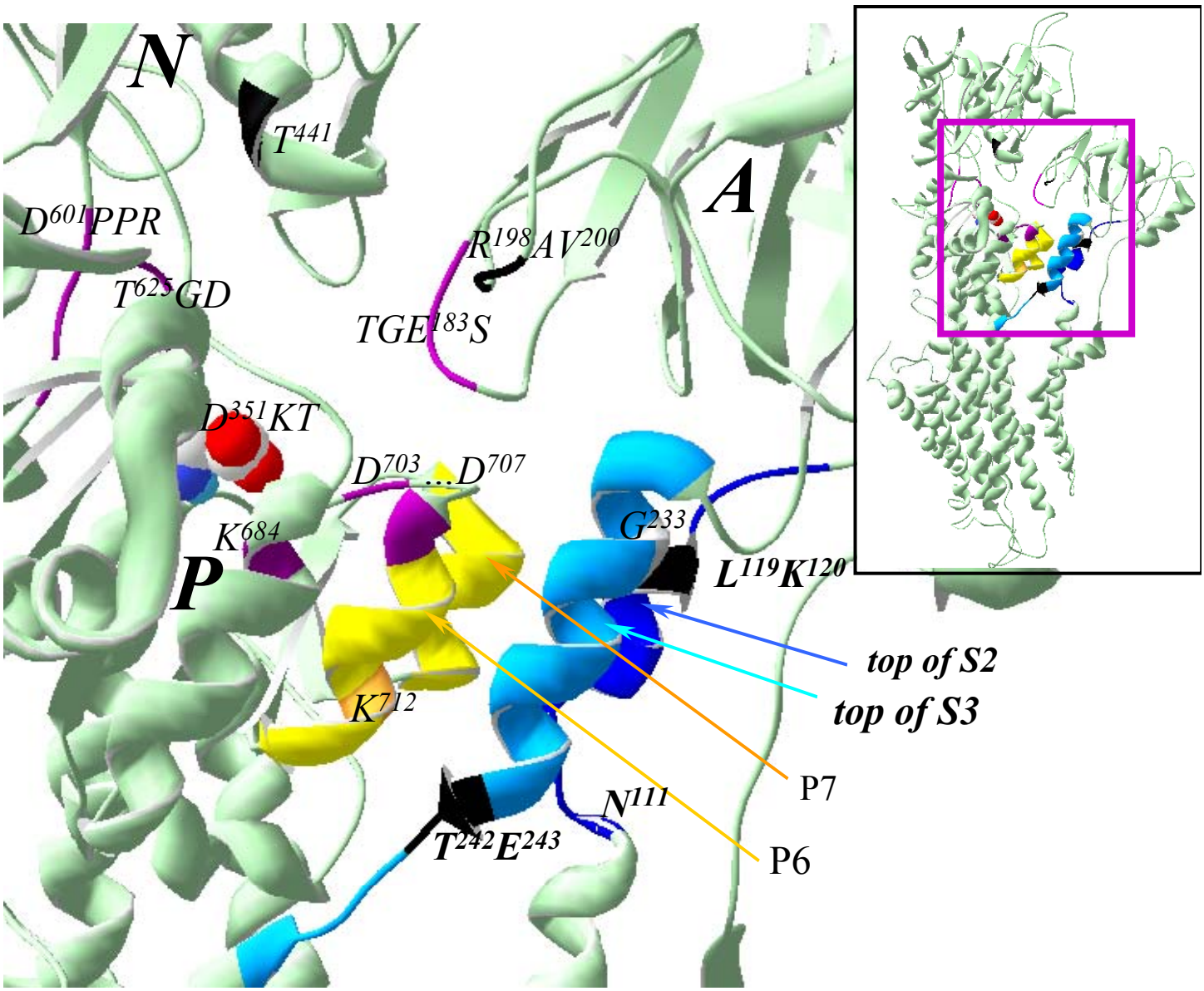

Fig 10_v4= 1IWO interface.ppt

SUPPLEMENTAL DATA

Figure "0". **Conditions for separation of proteolytic fragments and yet retention of phosphorylation.**

SR (about 8 µg per lane) and PK-treated SR (about 4 µg per lane) were first phosphorylated from Pi for 15 minutes at 20 °C in 25 % DMSO. Then, they were submitted to SDS-PAGE under different conditions: from left to right, (i) Sarkadi gels, 7 % acrylamide, run in the cold room; (ii) Sarkadi gels, 7 % acrylamide, run at room temperature; (iii) Laemmli gels, 12 % acrylamide in 1 mM Ca^{2+}, run at room temperature.

Note that in addition to ^{32}P labelling of intact ATPase (or large proteolytic bands), a very faint labelling by ^{32}P shows up in the region corresponding to M55 and calsequestrin in intact SR (0.5% of the labelling of intact ATPase; see dashed arrow). We do not know the origin of these few ^{32}P counts. The few other counts found on top of the gel presumably correspond to aggregated material.

20 µl aliquots of resuspended samples (i.e. amounts identical to those deposited for electrophoresis) were also counted simultaneously with the PhosphorImager, together with the dried gels, allowing easy comparison between the initial radioactivity of the phosphorylated sample and the one remaining associated with the protein band(s) after electrophoresis. Less than half of the former was lost during electrophoresis (data not shown; see also legend to Figure 2).

Figure 1bis. **SDS-PAGE evidence that p95C and p14N remain associated during size exclusion HPLC in the presence of detergent.**

Here, deoxycholate-purified Ca^{2+}-ATPase membranes (DOC-ATPase, *lane 2*), were treated for 10 minutes with Proteinase K (0.03 mg/ml PK, 2 mg/ml DOC-ATPase, 5 mM Mg^{2+}, 0.5 mM EGTA, 100 mM Mops at pH 6.8 and 20°C), in the additional presence of thapsigargin (50 µM). The presence of thapsigargin during PK treatment was found to result in increased formation of p95 at the expense of p83 and intact ATPase, which was helpful for these experiments (although it is useless for the functional studies described in the rest of this work). After PK arrest, addition of Ca^{2+} and centrifugation, resuspended membranes were solubilized by $C_{12}E_8$ ($C_{12}E_8$ to protein ratio was 10 to 1). After pelleting nonsolubilized material, the supernatant was applied to a 3000SW 0.75 x 30 cm HPLC column with an 0.75 x 6 cm guard column, equilibrated and eluted with 100 mM NaCl, 20 mM Tes-NaOH, 5 mM Mg^{2+}, 0.5 mM Ca^{2+} and 1 mg/ml $C_{12}E_8$ at pH 7. Eluted fractions were collected and aliquots were examined by SDS-PAGE on a 11 % Tricine gel *(Juul et al., 1995)*: *lanes 4 and 5* correspond to early fractions, containing aggregated material; *lanes 6 and 7* correspond to the peak fractions where monomeric ATPase elutes when the experiment is performed with uncleaved ATPase, and *lanes 8 and 9* correspond to later fractions, collected during the falling phase of this peak and therefore containing smaller size complexes. *Lane 3* corresponds to the initial sample applied to the column. *Lane 1* shows molecular mass standards.

Figure 1ter. **Cartoon representation of the fragments formed during PK-treatment in the absence of Ca^{2+}, and Western Blot analysis of these fragments.**

Top part, a cartoon illustrating the major peptides present after PK treatment in the absence of Ca^{2+}: p95C/p14N complexes together with p83C/p28N complexes and residual intact ATPase, and possibly also complexes resulting from more extensive proteolysis. For the sake of simplicity, this cartoon assumes that ATPase units are monomeric.

Central part, Western Blot analysis of proteinase K fragments after cleavage in the presence of Mg^{2+}, in the presence or absence of Ca^{2+}. Here, after 15 minutes treatment with proteinase K in the presence of either 0.3 mM Ca^{2+} + 0.5 mM AMP-PCP ("PCP"), 0.5 mM

EGTA ("EG") or 0.3 mM Ca^{2+} alone ("Ca"), proteolysis was arrested, and 0.8 µg of each PK-treated sample (together with intact membranes ("none") and molecular mass Kaleidoscope standards ("KMW", BioRad) was loaded onto a Laemmli gel (with Ca^{2+}) for electrophoresis. An 8 % acrylamide was chosen to maximize separation of the high molecular weight gragments. After transfer onto PVDF membranes, the separated peptides were immuno-characterized with antibodies against the N-terminus (1-15 residues, left; note that p14N does *not* show up because low molecular weight fragments had been allowed to run out of the gel), the C-terminus (985-994 residues, right), or the central portion (577-588, center) of the ATPase, as described in Møller et al., 2002. Note that, in contrast with the results previously obtained when proteolysis was performed in the absence of Mg^{2+} (see Fig 2C in Juul et al., 1995), p81N and p27/28C peptides, resulting from cleavage at Val^{734} or Val^{747} were not formed in detectable amounts. Cleavage at 734-747 is therefore probably not a primary site of cleavage. Note also that in the presence of Mg^{2+}, the slowing down by AMPPCP of ATPase proteolysis is quite obvious (Danko et al., 2001b; Møller et al., 2002; Ma et al., 2003).

For convenience, the *bottom part* of the Figure, taken from Fig 1, again schematises the identified points of primary cleavage and the various proteolytic products.

***Figure 1quater*. MALDI-TOF mass spectrometry analysis of the N-terminal p14N fragment, either intact or after further cleavage by trypsin.**

The exact identity of the p14N fragment was checked by MALDI-TOF. For the experiment illustrated in the *main Panel*, SR vesicles treated with PK were solubilized, run on an HPLC size exclusion column in the presence of detergent, and the fraction eluting at the position where of monomeric ATPase normally elutes was directly examined by MALDI-TOF mass spectrometry, as described under methods, with cytochrome c serving as an internal standard. A prominent peak at 13404 was found, nicely corresponding to the blocked 1-119 peptide, whose theoretical $[M+H^+]$ value is 13404.3. Nevertheless, as this value is very close to the one for another conceivable fragment of ATPase, peptide 120-243 (whose theoretical average $[M+H^+]$ value is 13402.4), we submitted the p14N fragment (cut off from an SDS-PAGE gel) to further degradation by trypsin, and analyzed the resultant low molecular weight tryptic peptides (*inset).* Among those, two fragments evidently arising from the 1-119 peptide were found: peptide Y^{36}-K^{47} (N-terminal cut after K^{35}) (whose theoretical monoisotopic $[M+H^+]$ value is 1343.6) and peptide S^{8}-R^{31} (N-terminal cut after K^{7}) (whose theoretical monoisotopic $[M+H^+]$ value is 2631.2). In addition, a prominent peak showed up at 815.25, which corresponds to the acetylated M^{1}-K^{7} peptide (whose theoretical monoisotopic $[M+H^+]$ value is 815.4) and confirms the blockade of the ATPase N-terminus.

***Figure 2bis*. Steady-state phosphorylation from ATP of the p95C/p14N complex occurs with roughly the same apparent affinity for Ca^{2+} as phosphorylation of intact ATPase or p83C/p28N.**

PK-treated membranes were diluted to 0.2 mg/ml protein in a final phosphorylation medium, on ice, consisting of buffer A supplemented with 5 µM [γ–^{32}P]ATP and either 2.95 mM EGTA and 0.06 mM Ca^{2+} (lane 2) or 0.95 mM EGTA and various total concentrations of Ca^{2+}, namely 0.06, 0.4, 0.74, 1.06, 2.1 and 10 mM, respectively (lanes 3-8). The phosphorylation reaction lasted for 30 s. Lane 1 contained molecular mass markers (LMW). Panel A shows the PhosphorImager scan. From this scan and from the Coomassie Blue staining ability of the various bands (Panel C), we computed the relative ability of the various bands to retain ^{32}P (Panel B, as in Fig 2B), taking the maximal phosphorylation level of intact ATPase band as 100 %.

Comment: The apparent affinity for Ca^{2+} is not very different for intact ATPase and for the two large peptides. However, since this assay is based on steady-state handling of ATP by the ATPase, the deduced apparent affinity for Ca^{2+} is *not* the true affinity for equilibrium Ca^{2+} binding (see main text). This will be discussed in relation to *Figs 6 & 6bis.*

Figure 3bis. **The transition from ADP-sensitive to ADP-insensitive EP (from Ca_2E1P to E2P) is reasonably fast in p95C, as in intact ATPase.**

PK-treated membranes were diluted to 0.1 mg/ml protein and permeabilized with calcimycin (A23187, at a final concentration of 1 µg/ml) in a final ice-cold phosphorylation medium consisting of 100 mM Tes-Tris (pH 8.25 at room temperature, probably corresponding to about pH 8.6 on ice), no potassium, 10 mM Mg^{2+}, 105 µM Ca^{2+} and 55 µM EGTA. The medium was supplemented with 5 µM [γ-^{32}P]ATP, and phosphorylation was stopped after various periods either by directly adding acid, to measure the total EP formed (lanes 2-5), or by first adding 5 mM EGTA and 1 mM ADP, and quenching with acid 5 seconds later (lanes 6-9). Lane 1 contained molecular mass markers (PSMW). Lane 10 (not shown) contained a control in which the acid quench was performed 30 s (instead of 5 s) after ADP/EGTA addition, to confirm that E2P dephosphorylation was slow under these circumstances. Panel A shows the PhosphorImager scan. From this scan and from the Coomassie Blue staining ability of the various bands (Panel C), we computed the relative ability of the various bands to retain ^{32}P, taking the maximal phosphorylation level of intact ATPase (at 40 s, lane 4) as 100 % (Panel B: left, total EP; right, ADP-insensitive "E2P"). Under these alkaline conditions, essentially all EP in p95C (squares) was ADP-insensitive E2P, as also found at pH 7 (see Fig 3B), but the rate of its appearance was apparently not significantly slowed down compared to intact ATPase (circles); in contrast, the Ca2E1P to E2P transition was slowed down for p83C (triangles), as expected (*Møller et al., 2002*).

Figure 4bis. **Phosphorylation from [^{32}P]Pi of the p95C/p14N complex in DMSO at 20°C is slow, and dephosphorylation upon Pi chase is also slow.**

The kinetics of phosphorylation by [^{32}P]Pi were measured at 20°C in buffer B supplemented with 25 % DMSO, 1 mM EGTA and 200 µM [^{32}P]Pi (lanes 2-5). After 12 min of such phosphorylation, dephosphorylation was triggered by adding 20 mM non-radioactive Pi to the same medium (with only 10 % resulting dilution of the sample, i.e. the DMSO concentration remained high), and the kinetics of dephosphorylation was measured (lanes 6-9). Lanes 1 -not shown- and 10 contained molecular mass markers (LMW and PSMW, respectively). Panel A shows the PhosphorImager scan. From this scan and from the Coomassie Blue staining ability of the various bands (Panel C), we computed the relative ability of the various bands to retain ^{32}P (Panel B), taking the phosphorylation level of intact ATPase after 300 s as 100 %. Circles: intact ATPase; squares, p95C peptide; triangles, p83C peptide.

Figure 5bis. **Phosphorylation from [^{32}P]Pi of the p95C/p14N complex occurs with quasi-normal affinity for Mg^{2+}, but inhibition by vanadate of E2P formation from Pi is less pronounced.**

PK-treated and resuspended membranes (about 1 mg/ml) were incubated at 20°C for 65 minutes in buffer B supplemented with 25 % DMSO, 1 mM EGTA, 200 µM [^{32}P]Pi, and either various concentrations of Mg^{2+} (lanes 1-6; lane 1, with "zero" Mg^{2+}, correspond to a sample where 0.5 mM EDTA was added), or 10 mM Mg^{2+} and various concentrations of ortho-vanadate (lanes 6-10). Panel A shows the PhosphorImager scan. From this scan and from the Coomassie Blue staining ability of the various bands (Panel C), we computed the relative ability of the various bands to retain ^{32}P (Panel B), taking the phosphorylation level of intact ATPase at 10 mM Mg^{2+} and no vanadate (lane 6) as 100 %. Circles: intact ATPase; squares, p95C peptide; triangles, p83C peptide.

Comment: (i) The design of the Mg^{2+}-dependence experiment was far from perfect, as we tested phosphorylation in a range of Mg^{2+} concentrations too high to precisely reveal the apparent affinity for Mg^{2+}; it is nevertheless clear that the apparent affinity of p95C for Mg^{2+} is not much shifted, whereas this is the case for p83C. (ii) The design of the vanadate-dependence experiment was more or less copied from a similar one in *Andersen and Vilsen*

1993, except that in our case there was no preincubation with vanadate before phosphorylation from Pi, but simple competition over 65 minutes. Interpretation of such an experiment is not straigthforward, because of interdependence between the reaction with Pi and the reaction with vanadate; but, as we previously found that the "true" affinity for Pi was similar for intact ATPase and p95C, the fact that vanadate proves to be a weaker apparent competitor of Pi for p95C than for intact ATPase must probably be assigned to a weaker true binding of vanadate. A more unambiguous assay of the true affinity of p95C for vanadate is shown in Fig 6.

***Figure 6bis*. Phosphorylation from [γ-^{32}P]ATP of the p95C/p14N complex, pre-equilibrated in a Ca^{2+}-deprived state, is also slow at 20°C.**

This experiment was similar to the one corresponding to lanes 2-4 in *Fig 6*, except that temperature was 20 °C. PK-treated membranes, initially at 0.4 mg/ml protein in buffer A supplemented with 200 µM EGTA, were mixed vol/vol with a medium containing 10 µM [γ–^{32}P]ATP and 300 µM Ca^{2+}, and acid-quenched after various periods in a rapid mixing-and-quenching equipment (hence the millisecond time scale). Lane 1 contained molecular mass markers (PSMW). Panel A shows the PhosphorImager scan. From this scan and from the Coomassie Blue staining ability of the various bands (Panel C), we computed the relative ability of the various bands to retain ^{32}P (Panel B), taking the phosphorylation level of intact ATPase at 30 s as 100 %. Circles: intact ATPase; squares, p95C peptide; triangles, p83C peptide. The lane labeled "9*" (or 600 ms*) is taken from the gel previously illustrated in *Fig 2* above, resulting from an experiment which was performed in parallel and in which ATP was added to Ca^{2+}-equilibrated membranes. The 600 ms* situation in that experiment is considered to be a fair estimate of the steady state situation to be obtained (hence the dotted lines in Panel B of the present Figure) when membranes are initially Ca^{2+}-free.

***Figure 10bis.* H-bonds between S2 and the rest of the ATPase in the various structures available for Ca^{2+}-depleted ATPase.**

Top: 1IWO; middle, 1FQU; bottom, 1KJU. The ATPase is viewed from the back relative to Fig 10. In this cartoon, residues 111-124 are colored dark blue, residues 230-247 are colored light blue, P6 and P7 are colored yellow. Bonds were predicted by SwissPDBViewer. NB: in the structure of Ca^{2+}-bound ATPase (1EUL, not shown), S2 interacts with S4 (on top of M4) via the Tyr^{122}-Arg^{324} and the Glu^{123}-Arg^{334} bonds.

Addendum to the Discussion: phosphorylation properties of the p83C peptide

It has been mentioned in the main text that the phosphorylation properties of the p83C peptide found in the present study were in nice agreement with those found in our previous study of the p83C/p28N complex (*Møller et al., 2002*). However, it has also been mentioned, and explicitly illustrated in the cartoon of Fig 1, that after ATPase treatment with PK in the presence of EGTA, it was certainly conceivable that not only singly cleaved but also *doubly cleaved* chains would show up, consisting of (p83C+p14N+p14b) complexes, coexisting with the singly cleaved p83C/p28N and p95C/p14N complexes. Two questions then arise, namely: (i) do these ternary complexes exist in significant amounts, and (ii) if these doubly cleaved chains are produced, what are their catalytic properties?

We think that the answer to question (i) is yes. There is no *a priori* reason for which a p95N/p14N complex would escape being cleaved once more, now at Glu^{243}, producing a (p83C+p14N+p14b) complex, and Fig 1 in fact provides two reasons for thinking so. Firstly, comparing lanes 7 and 8 shows that more p83C (and more p14N) has been formed after 15 minutes cleavage than after 5 minutes, but that the amount of p95C has not much changed, suggesting that p83C originates not only from primary cleavage of intact ATPase, but also from secondary cleavage of p95C at Glu^{243}. Secondly, the amounts of Coomassie Blue bound to the p95C and p83C peptides after 15 minutes (lane 8) are about in a 1:2 ratio, suggesting about the same 1:2 ratio in molar stoichiometry of the two peptides (as these two peptides have fairly similar masses); if p95C had *not* been able to undergo further cleavage at Glu^{243}, the molar amounts of p14N and p28N would then also be in the same 1:2 molar ratio, i.e. the protein masses in these bands corresponding to 14 and 28 kDa peptides would be in a 1:4 ratio, which is certainly not the case (it is closer to 1:1, see lane 8). Hence, it seems that a significant fraction of the p83C peptide complements an already cleaved (p14N+p14b) N-terminus instead of the primary cleavage product p28N.

The question then arises of whether the few existing (p83C+p14N+p14b) complexes gave rise to distinct features in our functional assays. In this respect, it is perhaps significant that in the present work, we were able to see very slow dephosphorylation of part of the p83C peptide (*Fig 3, and Fig 4bis in the present Supplemental Data* section). This could conceivable reveal the cut at L^{119}-K^{120}. It could however also be that in doubly cleaved ATPase, the three peptides do not always stay associated (in our previous work, p14b peptides were found both in the supernatant and in the pellet after centrifugation of PK-treated membranes, suggesting loose binding; see *Juul et al., 1995,* Table I), and the p83C peptides left solitary do no phosphorylate at all.

Fig 0 : Conditions for separation of proteolytic fragments and yet retention of phosphorylation.

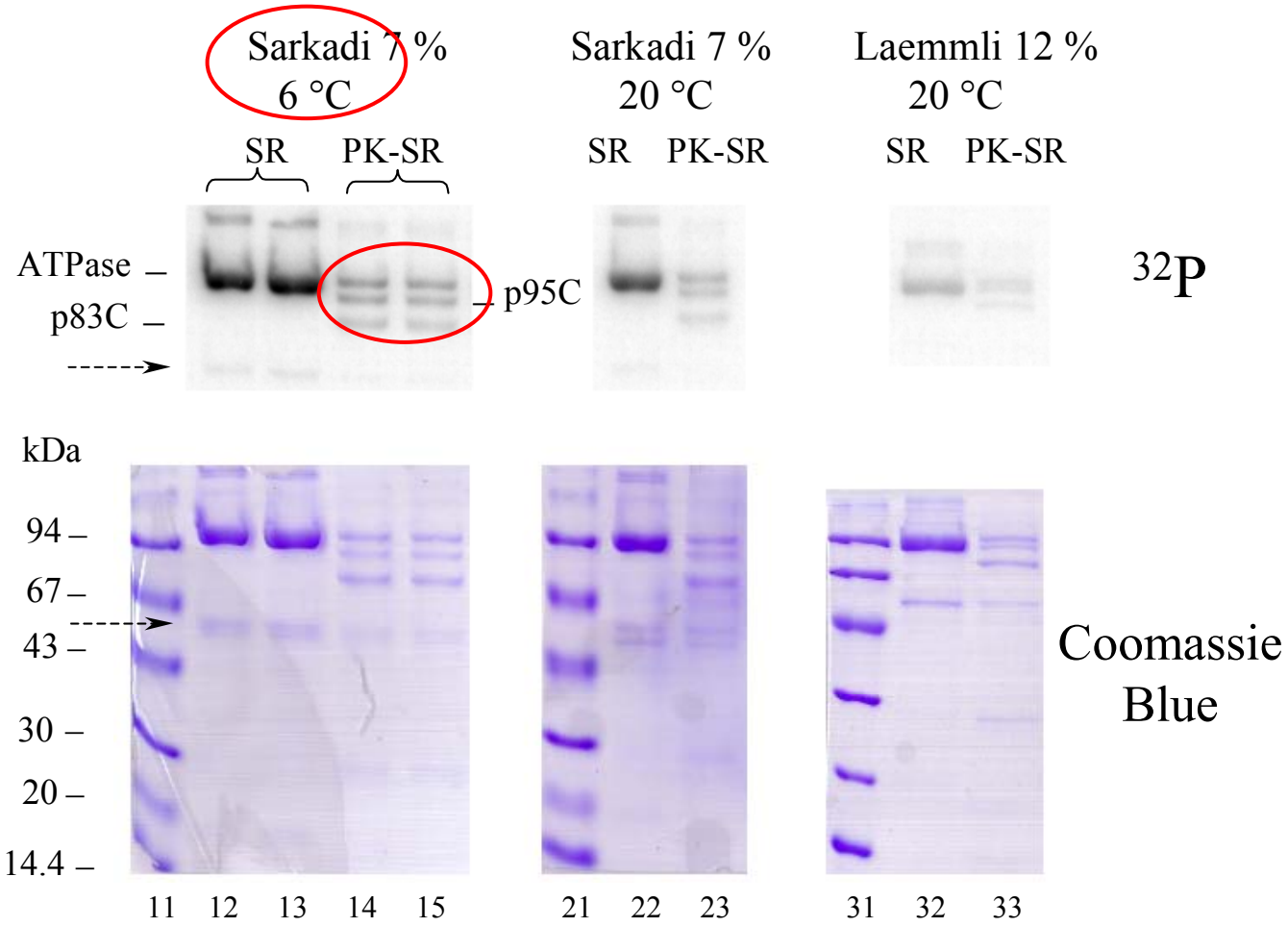

Figure 1bis. SDS-PAGE evidence that p95C and p14N remain associated during size exclusion HPLC in the presence of detergent.

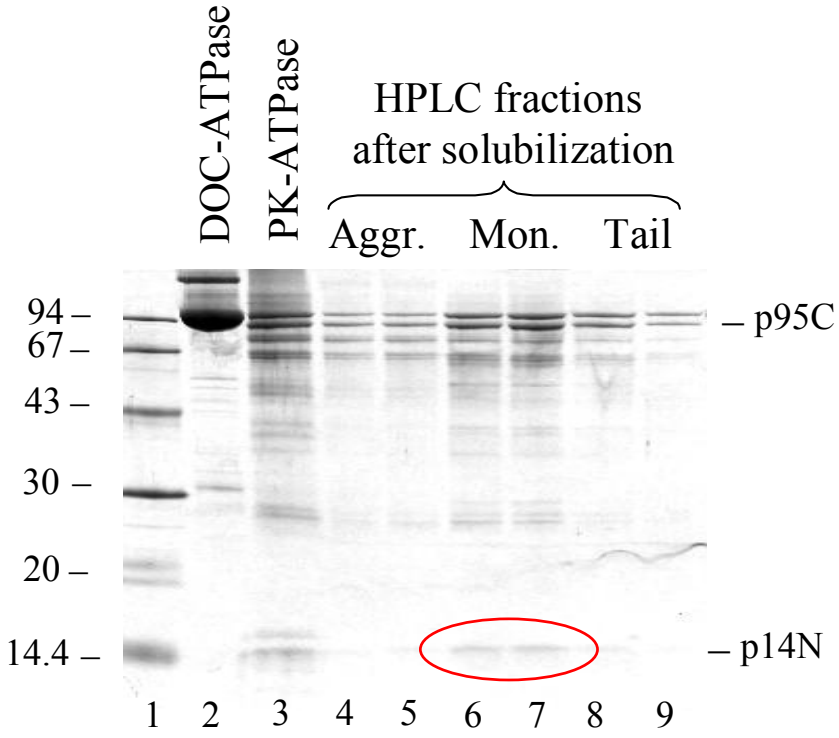

Fig 01bis_v4=030626_Bitten's expt Figure.ppt

Fig 1ter. Cartoon representation of fragments formed during PK-treatment in the absence of Ca^{2+}, and Western Blot analysis of fragments

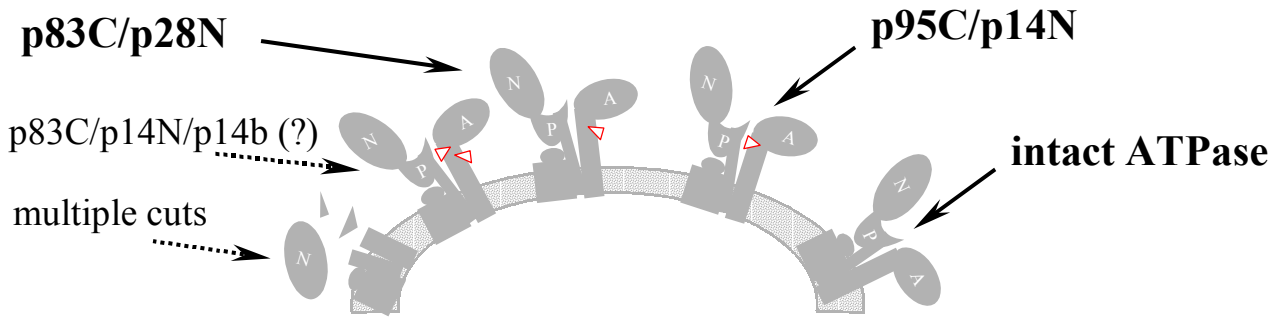

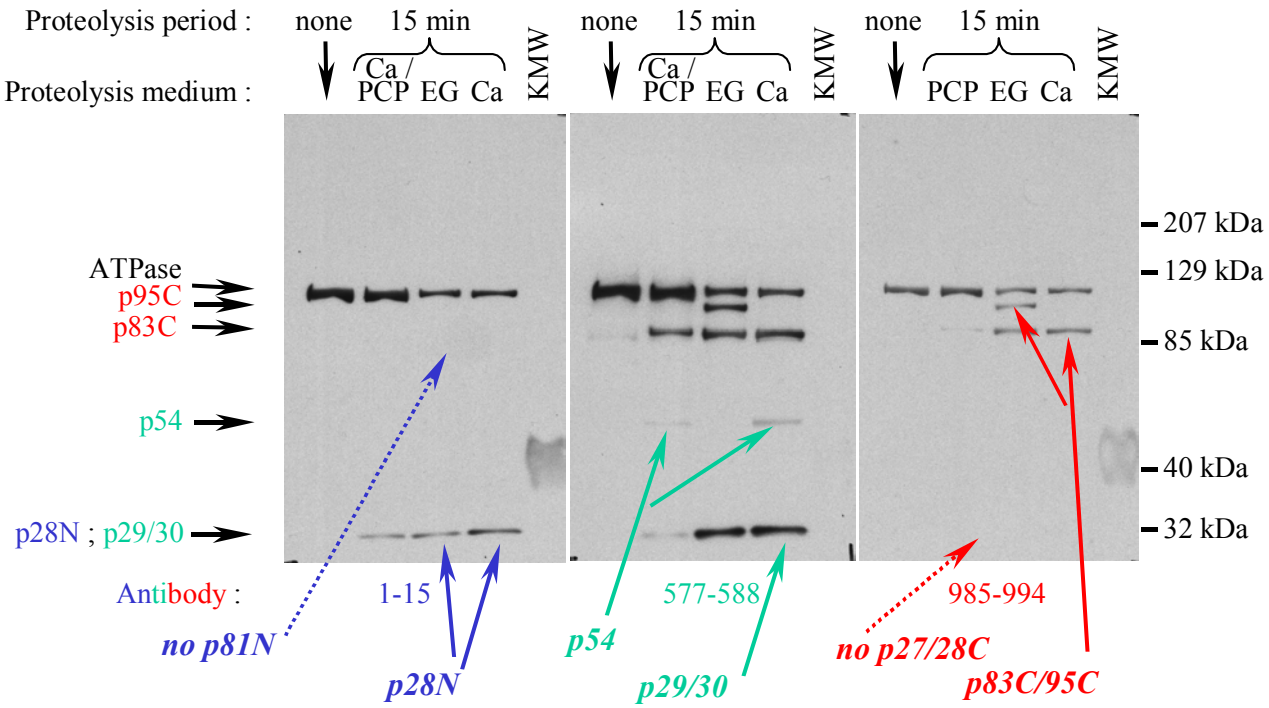

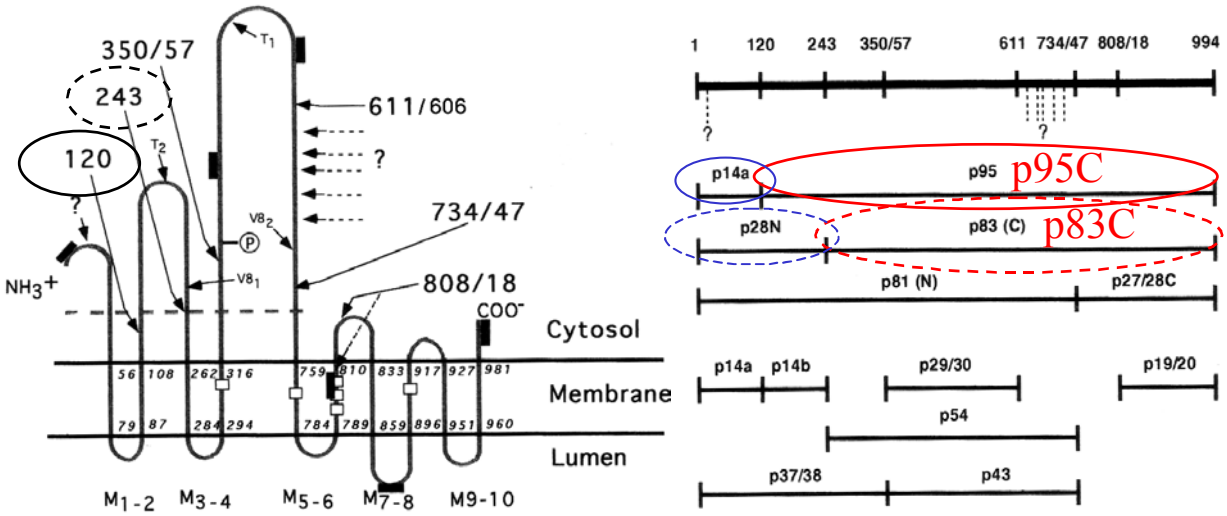

Fig 01ter_v4=cartoon + 030604 WB.ppt

Fig 1quater. Mass spectrometry analysis of the p14N fragment, either intact or after further cleavage by trypsin.

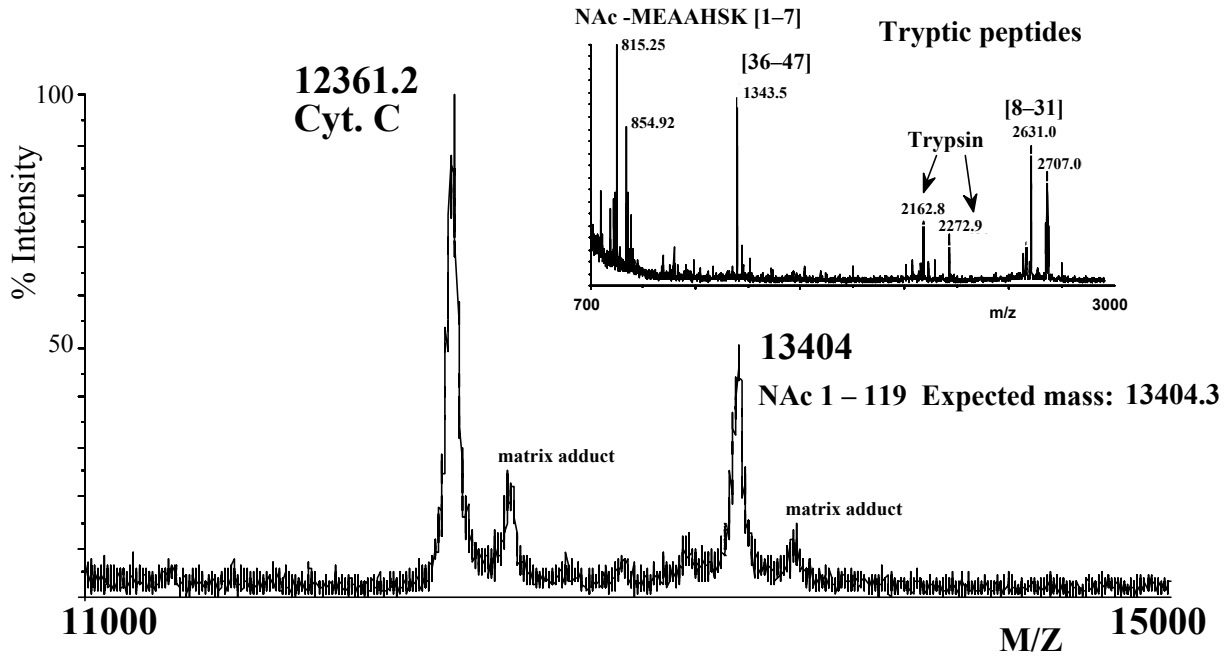

Fig 2bis. Phosphorylation from [γ-^{32}P]ATP of the p95C/p14N complex occurs at steady-state with roughly the same *apparent* affinity for Ca^{2+} as phosphorylation of intact ATPase or p83C/p28N.

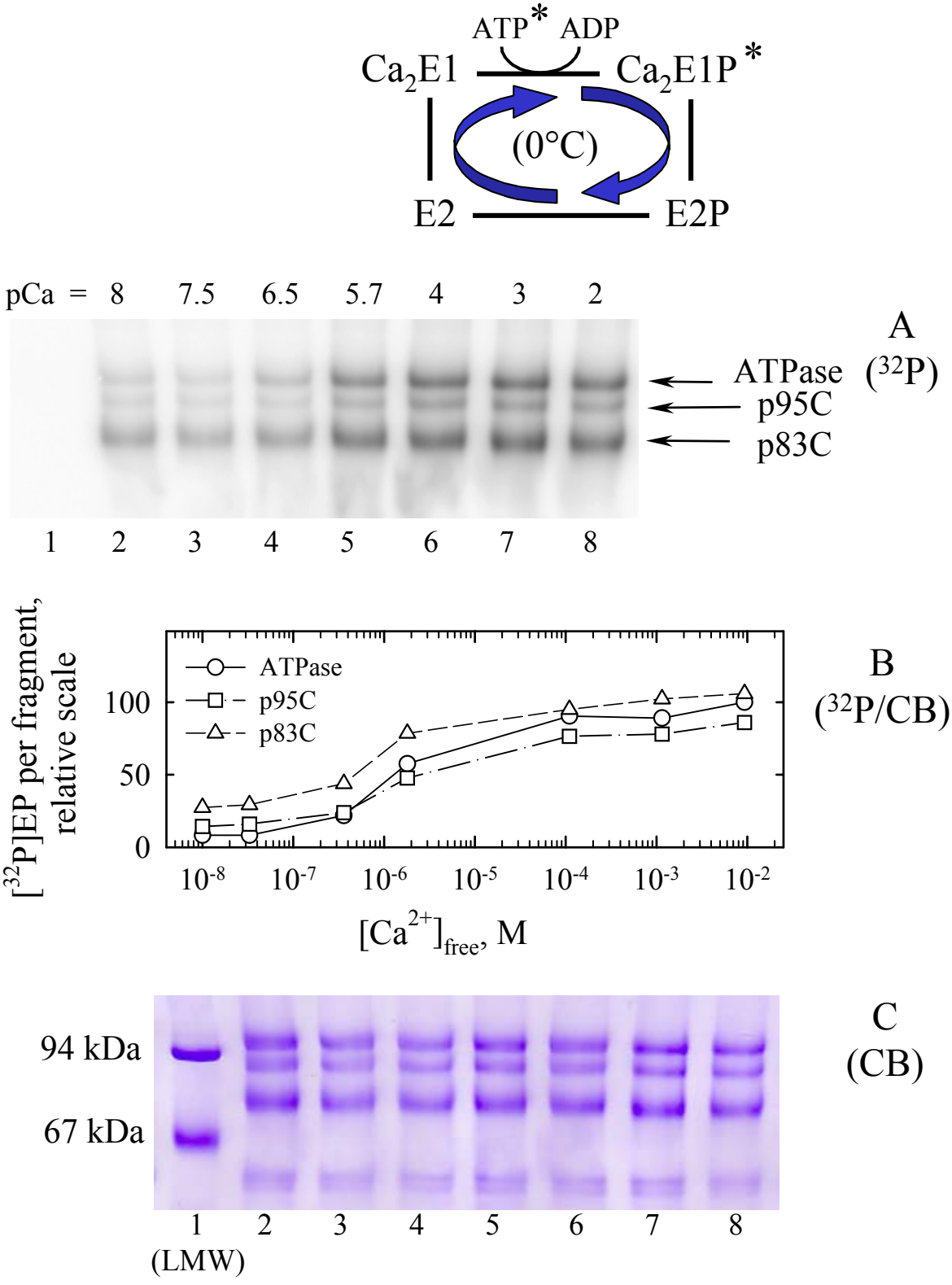

Fig 02bis_v4=p95 phosphorylation from ATP f(pCa).ppt (011024_d)

Fig 3bis. The transition from ADP-sensitive to ADP-insensitive EP (at 0°C, zero K^+ and alkaline pH) is reasonably fast in p95C as in intact ATPase (whereas that for p83C is slowed down).

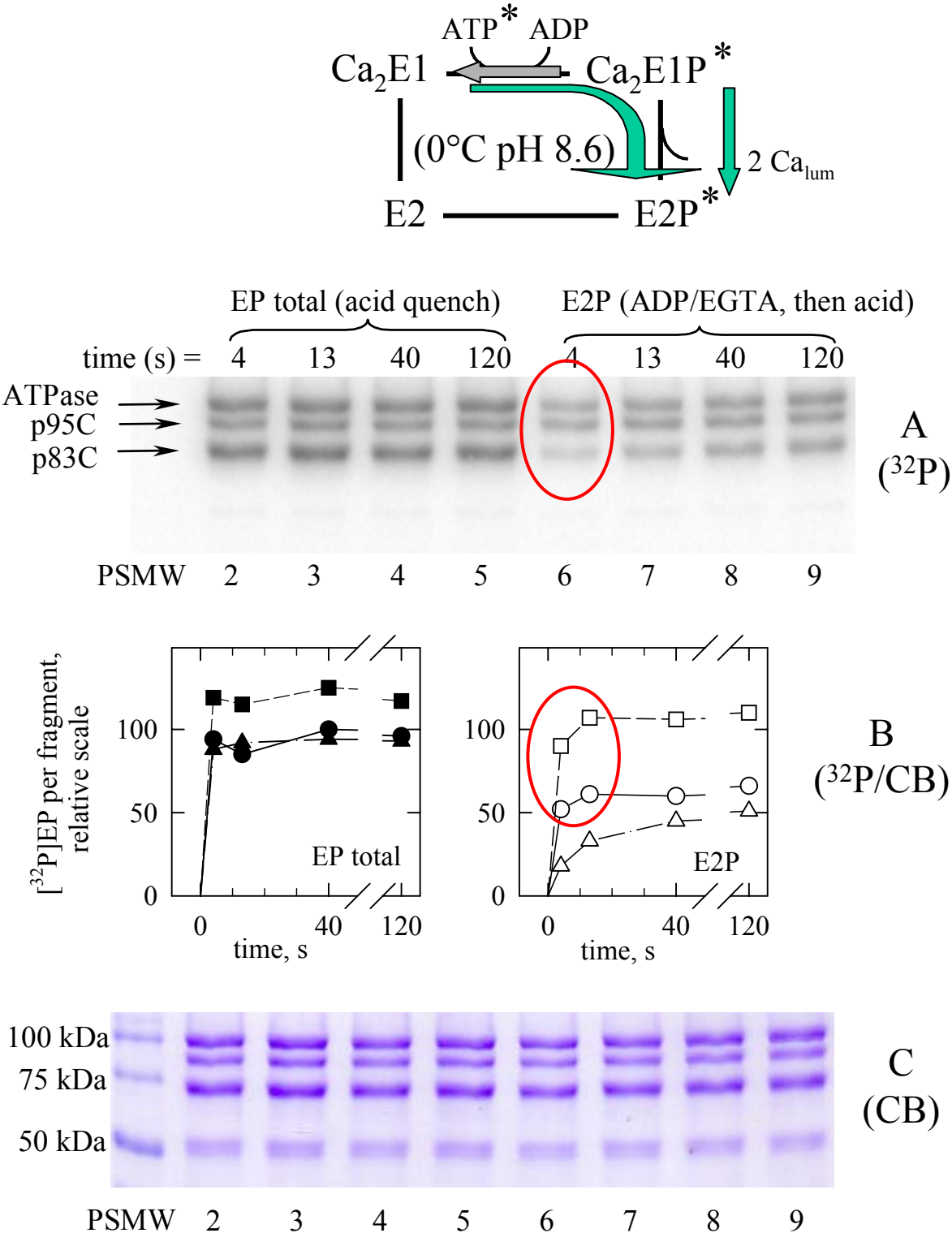

Fig 03bis_v4=from E1P to E2P_030612_d.ppt

Fig 4bis. Phosphorylation from [^{32}P]Pi of the p95C/p14N complex is slow in DMSO at 20°C, and dephosphorylation upon Pi chase is also very slow.

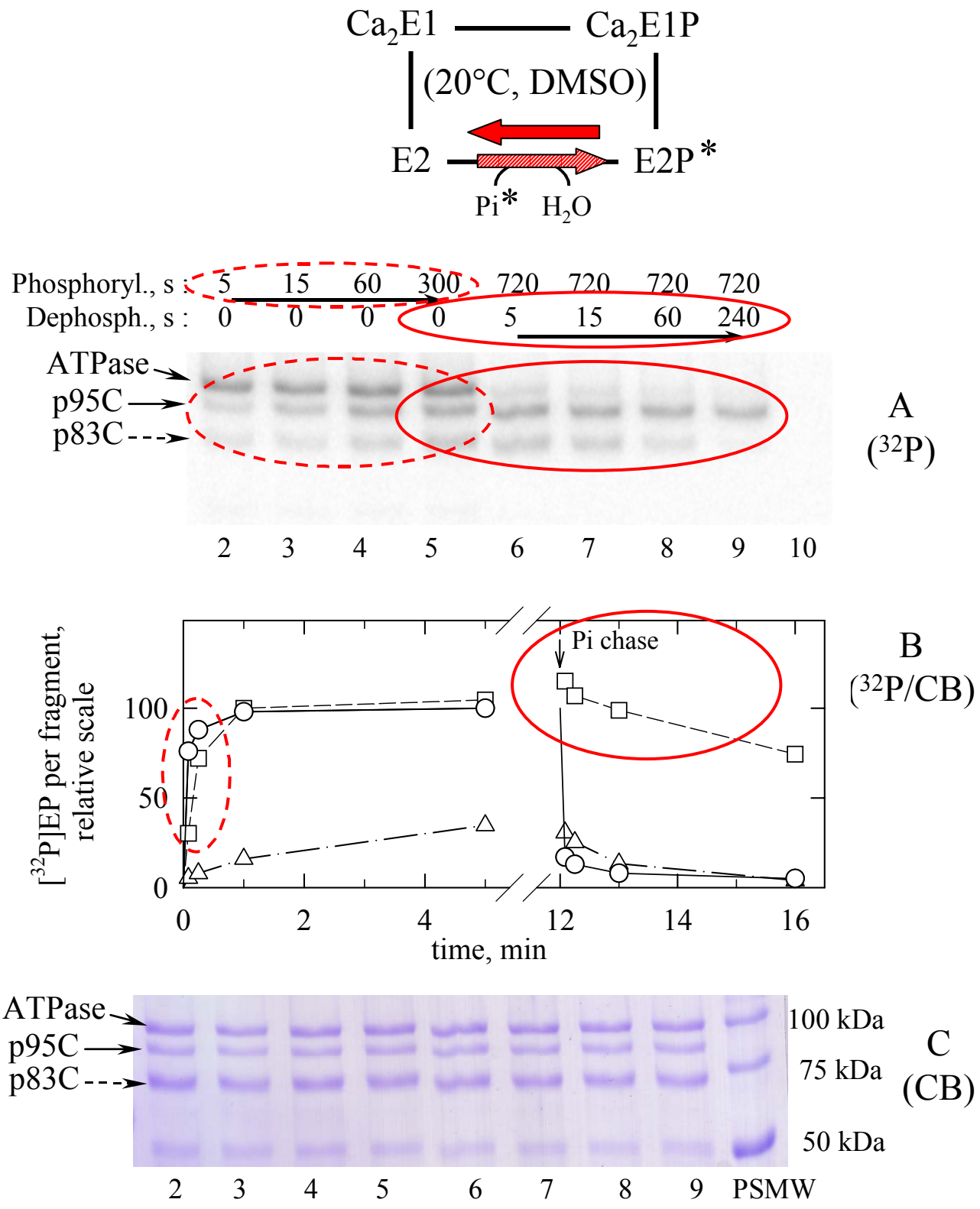

Fig 04bis_v4=kinetics of E2P dephosphorylation (and phosphor) in DMSO_030318b.ppt

Fig 5bis. Equilibrium phosphorylation from [^{32}P]Pi of the p95C peptide occurs with quasi-normal affinity for Mg^{2+}, but inhibition by VO_4 is less pronounced.

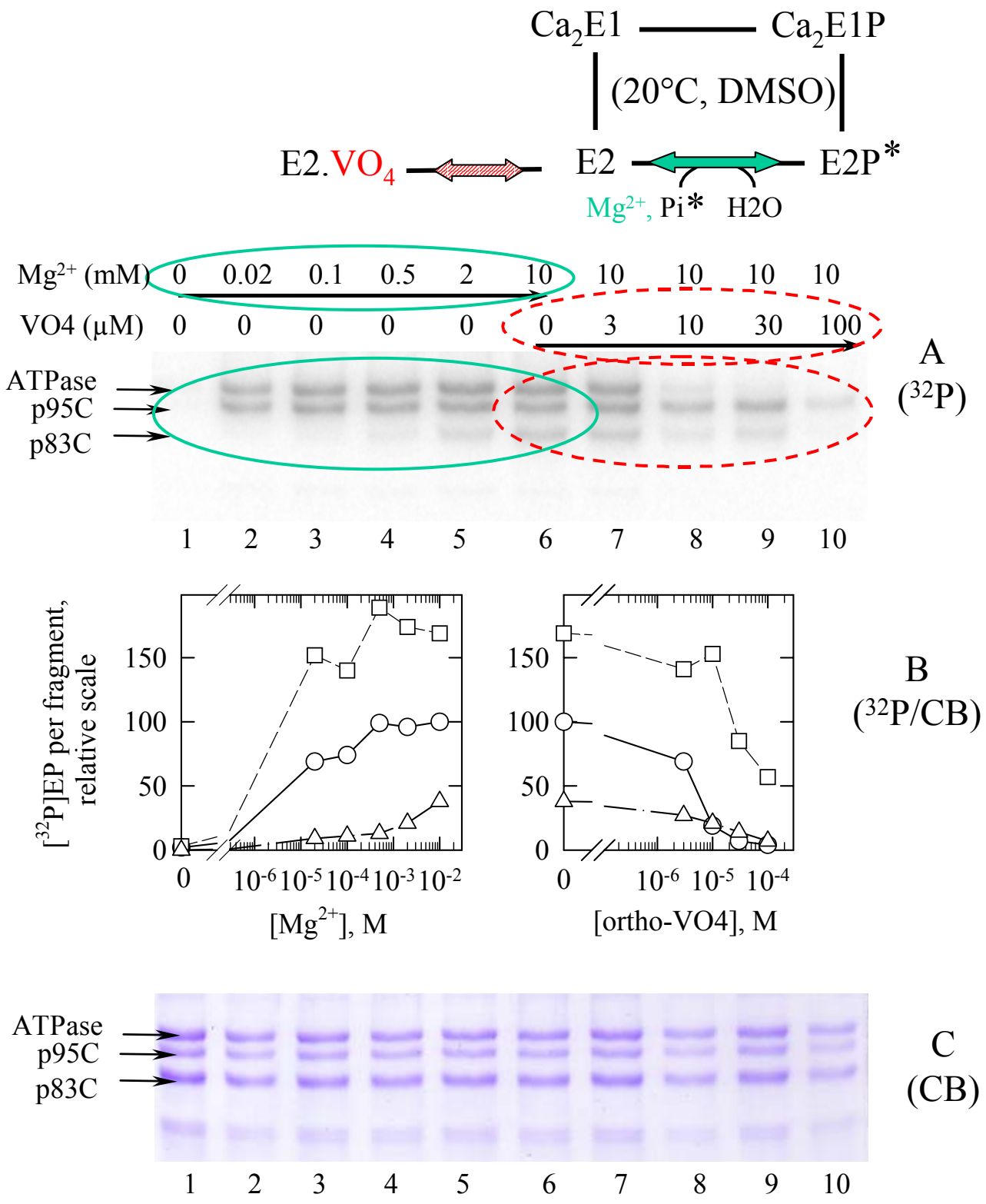

Fig 05bis_v4=E2P f(Mg) & f(VO4)_030612_a.ppt)

Fig 6bis. Slow phosphorylation from [^{32}P]ATP of the p95C/p14N complex at 20 °C following preequilibration of the enzyme in EGTA.

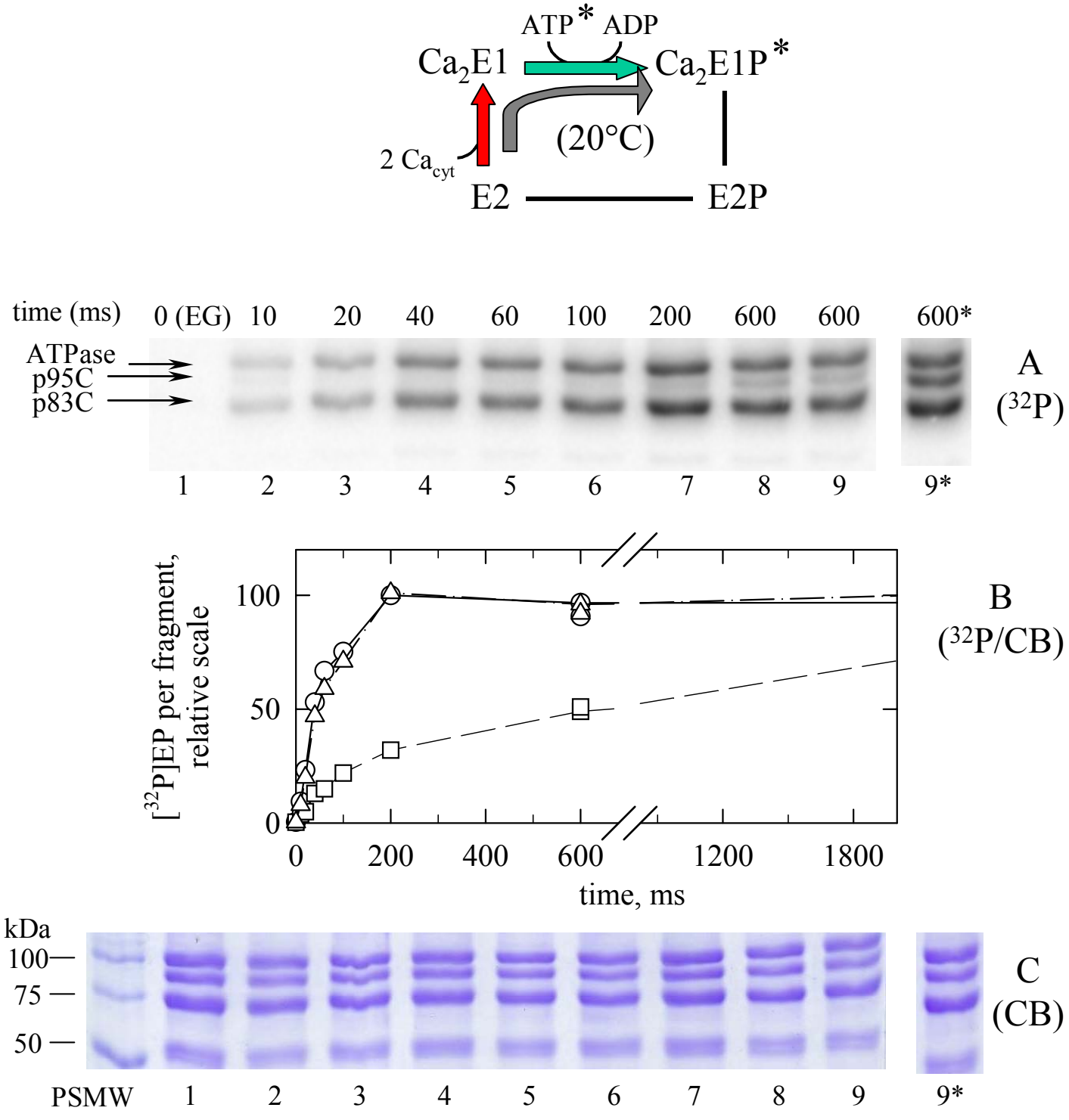

Fig 06bis_v4=QFM(EG)_030507

Fig 10bis. Predicted H-bonds in various structures….

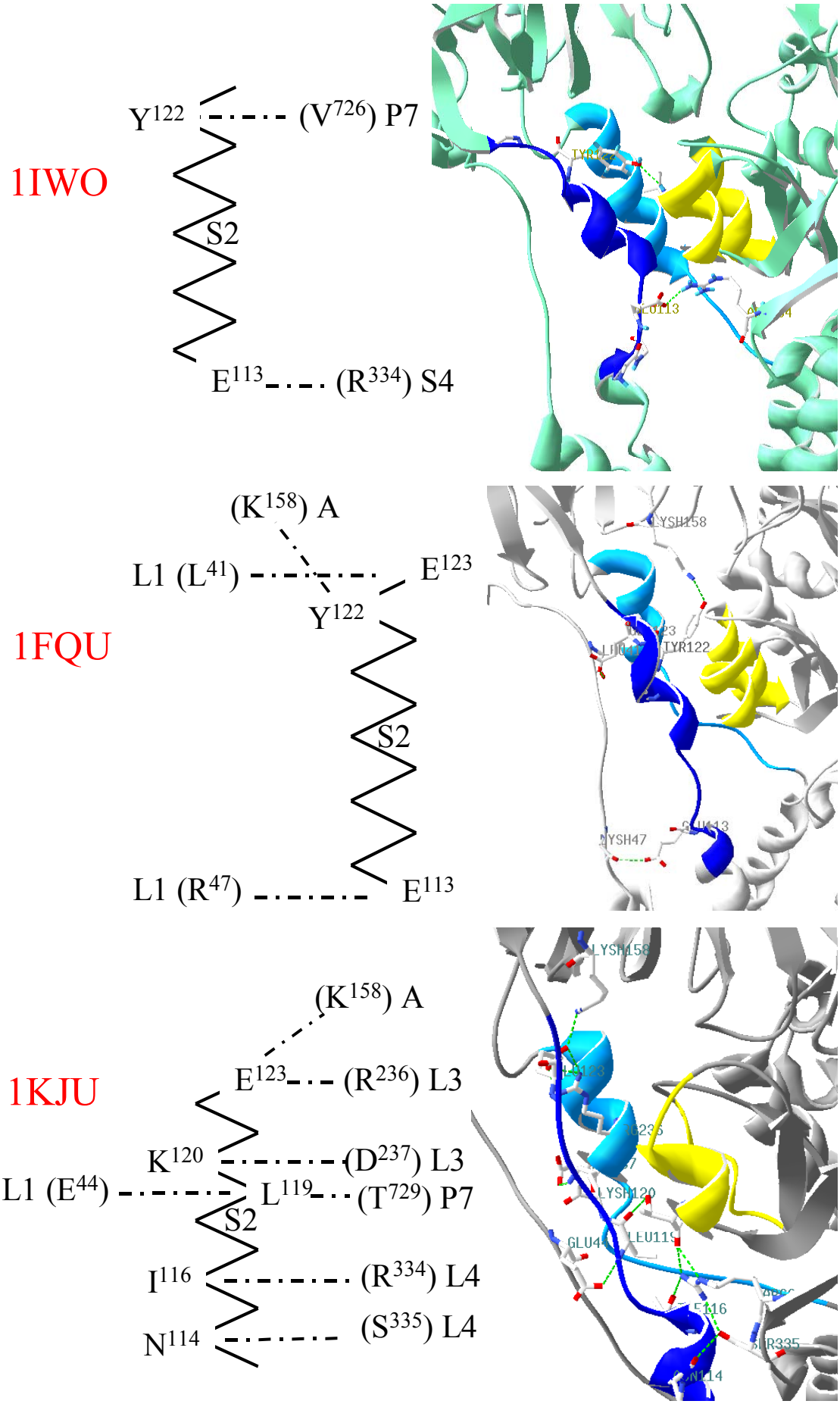

Fig 10bis_v4= H-bonds in various structures.ppt